In presenting the dissertation as a partial fulfillment of the requirements for an advanced degree from the Georgia Institute of Technology, I agree that the Library of the Institute shall make it available for inspection and circulation in accordance with its regulations governing materials of this type. I agree that permission to copy from, or to publish from, this dissertation may be granted by the professor under whose direction it was written, or, in his absence, by the Dean of the Graduate Division when such copying or publication is solely for scholarly purposes and does not involve potential financial gain. It is understood that any copying from, or publication of, this dissertation which involves potential financial gain will not be allowed without written permission.

_____

_____

3/17/65
b

ON THE PARAMETRIC INSTABILITY OF A CANTILEVER COLUMN WITH A SINUSOIDAL LONGITUDINAL END DISPLACEMENT

A THESIS

Presented to

The Faculty of the Graduate Division

by

Otis Halbert Burnside

In Partial Fulfillment

of the Requirements for the Degree

Master of Science in Engineering Mechanics

Georgia Institute of Technology

April, 1967

ON THE PARAMETRIC INSTABILITY OF A CANTILEVER COLUMN

WITH A SINUSOIDAL LONGITUDINAL END DISPLACEMENT

Approved:

Chairman

Date approved by Chairman: May 10, 1967

ACKNOWLEDGMENTS

The author wishes to thank Dr. Wilton W. King, whose direction as advisor made this thesis possible; Dr. Milton E. Raville, Dr. Edward R. Wood, and Dr. Charles E. S. Ueng for their reading of the thesis; and Mr. John C. Simonis and Mr. Stephen L. Passman for their help in the experimental work.

TABLE OF CONTENTS

Page

ACKNOWLEDGMENTS ii

LIST OF TABLES v

LIST OF ILLUSTRATIONS vi

LIST OF PRINCIPAL SYMBOLS viii

SUMMARY xi

Chapter

I. INTRODUCTION 1

A Statement of the Problem
A Brief Review of the Literature
An Approach to the Solution

II. LONGITUDINAL AND TRANSVERSE MOTION OF A CANTILEVER COLUMN 6

Derivation of the Equations of Motion
Longitudinal Vibrations of a Column
Free Transverse Vibrations of a Column

III. DERIVATION OF THE GOVERNING MATHIEU'S EQUATION 16

IV. ANALYTICAL DETERMINATION OF THE INSTABILITY REGIONS . . 22

Influence of Damping on the Instability Regions

V. THE EXPERIMENTAL PROCEDURE 26

Experimental Apparatus
Measurement of Damping
Experimental Determination of the Instability Regions

VI. RESULTS AND CONCLUSIONS 30

The Effect of Damping
Discussion of Farrell's [13] Results

TABLE OF CONTENTS (Continued)

Page

Appendices

I. EXPERIMENTAL OBSERVATIONS AND CALCULATIONS 40

II. COMPUTER METHODS AND RESULTS 59

LITERATURE CITED 92

LIST OF TABLES

Table		Page
1.	Experimental Second Mode Principal Instability Region for a 16 Inch Column	51
2.	Experimental Second Mode Principal Instability Region for a 35 Inch Column	53
3.	Experimental Third Mode Principal Instability Region for a 35 Inch Column	56

LIST OF ILLUSTRATIONS

Figure		Page
1.	Column System with End Excitation	2
2.	The Experimental Apparatus	27
3.	Analytical and Experimental Principal Instability Region for Second Mode Vibration	31
4.	Analytical and Experimental Principal Instability Region for Second Mode Vibration	32
5.	Analytical and Experimental Principal Instability Region for Third Mode Vibration	33
6.	The Influence of Damping on the First Three Analytical Regions of Instability	34
7.	Lines of Constant Amplitude Plotted on the First Mode Principal Instability Region	36
8.	Comparison to Farrell's Theoretical Undamped Principal Instability Region	38
9.	Comparison to Farrell's Theoretical Undamped Principal Instability Region	39
10.	Second Mode Unstable Configuration	41
11.	Third Mode Unstable Configuration	42
12.	The Relationship between the Bending Strain (Top) and the Base Displacement (Bottom) for Second Mode Instability	43
13.	The Relationship between the Bending Strain (Top) and the Base Displacement (Bottom) for Second Mode Instability	44
14.	The Relationship between the Bending Strain (Top) and the Base Displacement (Bottom) for Third Mode Instability	45
15.	Strain Trace of First Mode Damped Oscillations	46
16.	Strain Trace of Second Mode Damped Oscillations	47

LIST OF ILLUSTRATIONS (Continued)

Figure Page

17. Strain Trace of First Mode Damped Oscillations 48

18. Strain Trace of Second Mode Damped Oscillations 49

19. Strain Trace of Third Mode Damped Oscillations 50

LIST OF PRINCIPAL SYMBOLS

A_c	cross sectional area of column
A_ϵ	potential energy due to an external moment, shear force, and axial force at $x = \ell$
A_p	amplitude of base displacement
A,B,C,D	constants in the free vibration mode shape
$\bar{c}$	coefficient in Mathieu's equation
d	width of column
E	Young's modulus of column
e_c	distance of the center of gravity of the end mass from the end of the column
h	height of column
I	area moment of inertia of the column about a centroidal line parallel to the y axis
J	mass moment of inertia of the end mass about a centroidal line parallel to the y axis
k	$\left(\frac{\omega_n^2 \rho A_c}{EI}\right)^{\frac{1}{4}}$
ℓ	length of column
m	mass of end mass
M(x,t)	bending moment in the y direction
n	integer referring to the nth mode of free vibration
P(x,t)	axial force in column
Tn(t)	undetermined functions in Galerkin's analysis

T	kinetic energy of the column
t	time
U	internal energy of the column
$u(x,t)$, $v(x,t)$, $w(x,t)$	displacements of a point on the column in the x, y, and z directions respectively
$V(x,t)$	shear force in the z direction
x,y,z	coordinates defining the position of particles relative to one end of the column
α, β, γ	coefficients in Mathieu's equation determined by the Galerkin analysis
Δ_n	damping decrement for the nth mode of free vibration
$\delta(\quad)$	first variation of $(\quad)$
$\epsilon_i(x,t)$	error function in Galerkin's analysis
ϵ_n	coefficient of damping for the nth mode of free vibration
ϵ_x	axial strain
$\theta_n(x)$	functions which satisfy the same boundary conditions as $w(x,t)$
μ	$-\frac{\bar{c} A_p \Omega^2}{2 \omega_n^2}$
ρ	mass per unit volumn of column
σ_x	axial stress
$\psi_n(x)$	nth mode shape of free transverse vibration
$\Psi(x,t)$	$\psi_n(x) e^{i\omega_n t}$

ω_n	nth natural frequency of free vibration
Ω	frequency of base displacement
Ω_{*1}, Ω_{*2}, Ω_{*3}	first, second, and third damped instability boundaries

Dots over variables indicate differentiation with respect to time.

SUMMARY

Analytical and experimental principal instability regions were determined for the straight configuration of a cantilever column with a sinusoidal longitudinal displacement at its end. Columns investigated in the experimental part were shown to exhibit nearly rigid-body motion in the longitudinal direction while in the straight form. To establish a stability criterion for the straight column, a one-term Galerkin analysis was used to find a solution for the differential equation of transverse vibration. The assumed function satisfying the boundary conditions was taken to be a mode of free transverse vibration of the column with no longitudinal force. The Galerkin analysis yielded a Mathieu equation from which the instability boundaries could be found. The effects of viscous damping were also included in the theoretical analysis.

An experimental investigation was conducted to determine the principal regions of instability. The agreement between the experimental and theoretical results is excellent, and it can be concluded that the one-term Galerkin analysis is sufficient for the columns considered in this thesis.

CHAPTER I

INTRODUCTION

A Statement of the Problem

This paper investigates one of the many types of problems which arise in the study of dynamic stability of elastic systems. The system under consideration is a cantilever column excited at one end by a sinusoidal longitudinal displacement. Figure 1 shows the column and the manner in which the excitation is applied. It is observed experimentally, that for a given column, when certain relationships between the excitation frequency Ω and the amplitude A_p are satisfied, the column will exhibit transverse motion.

The classical buckling of a "flagpole" [1] is the static analogy to this problem. There, it is desired to know how high a vertical cantilever column can be raised without buckling under its own weight. The term "buckling" is used in the kinetic sense here. Suppose the straight column is given a perturbation of lateral displacement which produces small vibrations. If these vibration amplitudes are arbitrarily small for arbitrarily small disturbances, the straight configuration of the column is said to be stable; otherwise, the straight configuration is said to be unstable. The essence of the "flagpole problem" is not changed if the axial load arises from a constant axial acceleration of the column. The question is now: a given column must be subjected to what acceleration for it to buckle?

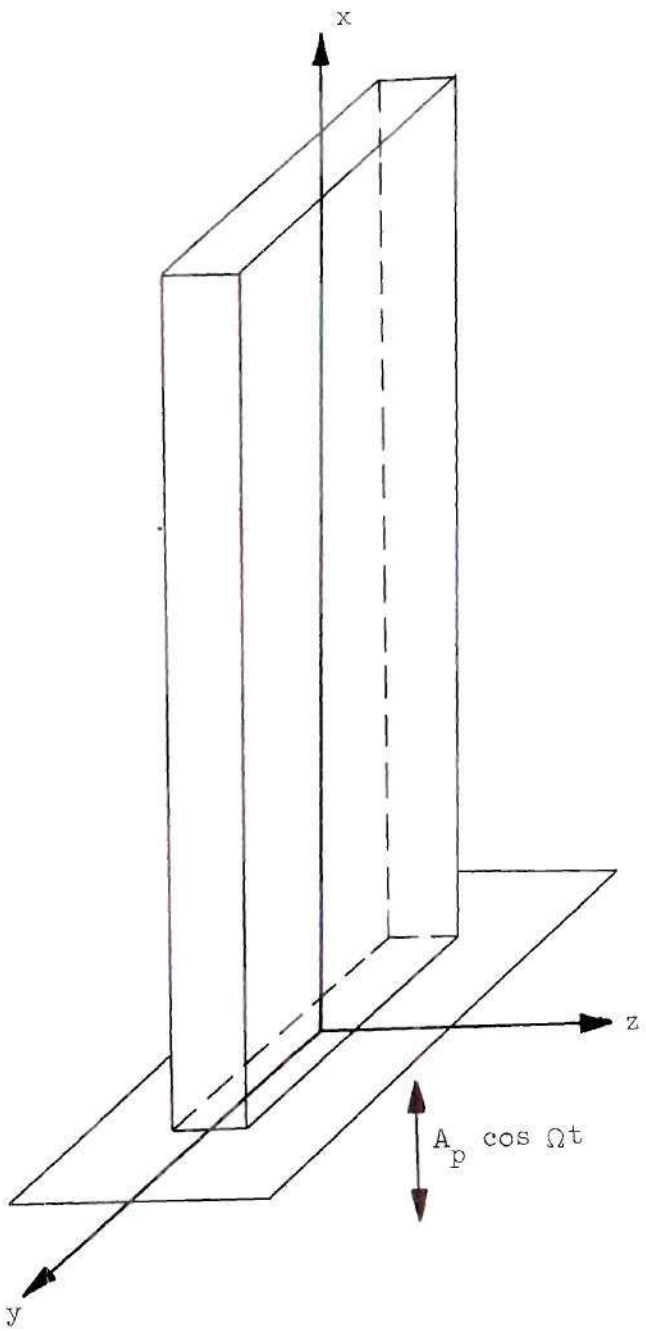

Figure 1. Column System with End Excitation.

If this acceleration is applied by a longitudinal end displacement $A_p \cos \Omega t$, the previous problem becomes the problem under investigation. Stoker [2] points out that since there are so many classes of stability problems for physical systems, no universally accepted definition of the term stability is possible. Each system will have its own stability criterion. Stability is defined for the system presented in this thesis in the following manner. Suppose $\xi(x,t)$ is the straight configuration of the column, exhibiting sinusoidal motion in the longitudinal direction, and let $\rho(x,t)$ be a displacement in the z direction measured from $\xi(x,t)$. The undisturbed motion $\xi(x,t)$ is said to be stable in the sense of Lyapunoff [3]* if for every $\epsilon>0$, no matter how small, there exist positive numbers $\eta_1(\epsilon)$ and $\eta_2(\epsilon)$ such that

$$|\rho(x,t)| < \epsilon$$

and $$|\dot{\rho}(x,t)| < \epsilon \quad \text{for } t > t_0 \qquad (1)$$

whenever $$|\rho(x,t_0)| < \eta_1(\epsilon)$$

$$|\dot{\rho}(x,t_0)| < \eta_2(\epsilon).$$

All straight configurations $\xi(x,t)$ which do not satisfy this criterion are called parametrically unstable. The term "parametrically unstable" means the column exhibits unstable lateral motion while being excited in a direction perpendicular to this motion. The basic problem examined in this paper consists in answering the following question: For given column parameters, displacement frequency Ω and displacement amplitude A_p, will the system become parametrically unstable?

*See Koiter [4] and Malkin [5] for the specialization of Lyapunoff's general definition of stability to the stability of equilibrium of continuous systems.

A Brief Review of the Literature

Beliaev [6] was the first to investigate (in 1924) the dynamic stability of elastic columns. The system he examined was a column simply supported at both ends and subjected to a time-dependent longitudinal force $P_1 \cos\gamma t$. If the axial force is considered constant along the column, small deflection beam theory yields a Mathieu equation:

$$\frac{d^2 f(t)}{dt^2} + (\lambda_1 - \mu_1 \cos\gamma t)\, f(t) = 0 , \qquad (2)$$

where $f(t)$ is the function of time in the lateral deflection equation. It is shown in the literature, such as in McLachlan [7], that equation (2) will have solutions which are unbounded in time if certain relationships exist between the coefficients λ_1 and μ_1. These unbounded or unstable points plot into entire regions in the λ_1 and μ_1 parameter space. The column variables, P_1, and γ are contained in λ_1 and μ_1 for the problem Beliaev analyzed.

The early work in this area was entirely Russian, and the first non-Russian paper on the dynamic stability of elastic systems did not appear until the late thirties. Reference [8] gives a survey of these Russian works through about 1952. Unfortunately, the amount of literature available in English is limited, but an important book by Bolotin [9] has been translated from the Russian. Beliaev's problem has been extended in recent analytical and experimental investigations [10, 11] to include the effect of damping, nonlinear elasticity, and longitudinal inertia on the instability regions. Weingarten [12] was able to obtain experimentally instability regions other than the principal region.

A study of the problem posed in this thesis was presented in late 1965 by Farrell [13]. However, there is a significant difference in the two methods of solution. A brief discussion of Farrell's paper is given in Chapter VI.

The dynamic stability of columns is only one of the areas in which investigations of dynamic stability of elastic systems are being conducted. Other areas include the stability of plates, shells, frames, and arches.

An Approach to the Solution

The basic difference between this paper and those previously presented on the dynamic stability of columns enters in the method of applying the axial force. The sinusoidal displacement at the end $x = 0$ creates an axial force which varies along the length of the column. Most of the other works on the subject consider the axial force a constant along the column.

Retention of certain non-linear terms in the strain-displacement equations of elasticity leads to a set of coupled differential equations for the transverse and longitudinal vibrations of the column in Figure 1. A possible solution to the system of coupled equations is $w(x,t) = 0$, the straight configuration. In order to determine conditions for stability of the straight configuration, a one-term Galerkin analysis is applied to the linear differential equation governing small transverse oscillations about the harmonic longitudinal motion. The assumed functions in the analysis which satisfy the boundary conditions are the modes of free vibration of a cantilevered column. The Galerkin analysis yields a Mathieu's equation for determining the boundaries of instability.

An experimental determination of the instability regions is also included in this study. The experimental analysis serves to check the validity of the one-term Galerkin analysis using the mode of free vibration.

CHAPTER II

LONGITUDINAL AND TRANSVERSE MOTION OF A CANTILEVER COLUMN

Derivation of the Equations of Motion

Consider that the column in Figure 1 will exhibit vibrations only in the x and z directions. Furthermore, make the following assumptions:

1) The column material is perfectly elastic and obeys Hooke's Law.
2) All stresses except σ_x are absent.
3) Lateral contractions are neglected.
4) Rotational inertia of the column is neglected.

The kinetic energy of the column is

$$T = \frac{1}{2} \int_o^{\ell} \rho A_c [\dot{u}^2 + \dot{w}^2] dx \ .$$

The internal energy of the column is

$$U = \frac{1}{2} \int_o^{\ell} EI\left(\frac{1}{R}\right)^2 dx + \frac{1}{2} \int_o^{\ell} EA_c \epsilon_x^{\ 2} \ dx \ ,$$

where R is the radius of curvature of the column, and ϵ_x is the axial strain. From the theory of elasticity

$$\epsilon_x = \frac{\partial u}{\partial x} + \frac{1}{2}\left[\left(\frac{\partial u}{\partial x}\right)^2 + \left(\frac{\partial v}{\partial x}\right)^2 + \left(\frac{\partial w}{\partial x}\right)^2\right]. \qquad (3)$$

By assuming that $\left(\frac{\partial u}{\partial x}\right)^2$ is small compared to $\frac{\partial u}{\partial x}$ and that $\frac{\partial v}{\partial x}$ is zero, equation (3) yields

$$\epsilon_x = \frac{\partial u}{\partial x} + \frac{1}{2}\left(\frac{\partial w}{\partial x}\right)^2 .$$

Also if the lateral slope is small compared to unity,

$$\frac{1}{R} = \frac{\partial^2 w}{\partial x^2} .$$

The potential energy due to an external moment, shear force, and axial force at $x = \ell$ is

$$A_\varepsilon = -M(\ell,t)\,\frac{\partial w}{\partial x}(\ell,t) - V(\ell,t)w(\ell,t) - P(\ell,t)u(\ell,t) .$$

Hamilton's Principle requires

$$\delta\int_{t_o}^{t_1} (U - T + A_\varepsilon)dt = 0 .$$

That is,
$$\delta\int_{t_o}^{t_1} \left\{\left[\frac{1}{2}\int_o^\ell EI\left(\frac{\partial^2 w}{\partial x^2}\right)^2 + EA_c\left(\frac{\partial u}{\partial x} + \frac{1}{2}\left(\frac{\partial w}{\partial x}\right)^2\right)^2 \right.\right.$$

$$\left.\left. - \rho A_c(\dot{u}^2+\dot{w}^2)\right]dx - M(\ell,t)\,\frac{\partial w}{\partial x}(\ell,t) - V(\ell,t)w(\ell,t) - P(\ell,t)u(\ell,t)\right\}dt = 0.$$

Taking E, I, A_c, and ρ as constants and following the usual procedures of the calculus of variations,

$$\int_{t_o}^{t_1} \left\{\int_o^\ell \left[EI\,\frac{\partial^2 w}{\partial x^2}\,\delta\,\frac{\partial^2 w}{\partial x^2} + EA_c\left(\frac{\partial u}{\partial x} + \frac{1}{2}\left(\frac{\partial w}{\partial x}\right)^2\right)\left(\delta\,\frac{\partial u}{\partial x} + \frac{\partial w}{\partial x}\,\delta\,\frac{\partial w}{\partial x}\right) - \rho A_c(\dot{u}\,\delta\dot{u}+\dot{w}\,\delta\dot{w})\right]dx \right.$$

$$\left. - M(\ell,t)\,\delta\,\frac{\partial w(\ell,t)}{\partial x} - V(\ell,t)\,\delta w(\ell,t) - P(\ell,t)\,\delta u(\ell,t)\right\}dt =$$

$$\int_{t_o}^{t_1} \left\{\int_o^\ell EI\,\frac{\partial^4 w}{\partial x^4}\,\delta w\,dx + EI\left(\frac{\partial^2 w}{\partial x^2}\,\delta\,\frac{\partial w}{\partial x} - \frac{\partial^3 w}{\partial x^3}\,\delta w\right)\Big|_o^\ell \right.$$

$$\left. - \int_o^\ell \frac{\partial}{\partial x}\left(EA_c\left(\frac{\partial u}{\partial x} + \frac{1}{2}\left(\frac{\partial w}{\partial x}\right)^2\right)\right)\delta u\,dx + EA_c\left(\frac{\partial u}{\partial x} + \frac{1}{2}\left(\frac{\partial w}{\partial x}\right)^2\right)\delta u\Big|_o^\ell\right.$$

$$- \int_o^{\ell} \frac{\partial}{\partial x}\left(EA_c \frac{\partial w}{\partial x}\left(\frac{\partial u}{\partial x} + \frac{1}{2}\left(\frac{\partial w}{\partial x}\right)^2\right)\right)\delta w \, dx + EA_c \frac{\partial w}{\partial x}\left(\frac{\partial u}{\partial x} + \frac{1}{2}\left(\frac{\partial w}{\partial x}\right)^2\right)\delta w\Big|_o^{\ell}$$

$$+ \int_o^{\ell} \rho A_c(\ddot{u}\delta u + \ddot{w}\delta w)dx - M(\ell,t)\delta\frac{\partial w}{\partial x}(\ell,t) - V(\ell,t)\delta w(\ell,t) - P(\ell,t)\delta u(\ell,t)\Big\}dt$$

$$- \int_o^{\ell} \rho A_c\left(\dot{u}\delta u\Big|_{t_o}^{t_1} + \dot{w}\delta w\Big|_{t_o}^{t_1}\right)dx = \int_{t_o}^{t_1}\Big\{\int_o^{\ell}\Big[EI\frac{\partial^4 w}{\partial x^4} - \frac{\partial}{\partial x}\left(EA_c\frac{\partial w}{\partial x}\left(\frac{\partial u}{\partial x} + \frac{1}{2}\left(\frac{\partial w}{\partial x}\right)^2\right)\right)$$

$$+ \rho A_c\ddot{w}\Big]\delta w \, dx + \int_c^{\ell}\Big[- \frac{\partial}{\partial x}\left(EA_c\left(\frac{\partial u}{\partial x} + \frac{1}{2}\left(\frac{\partial w}{\partial x}\right)^2\right)\right) + \rho A_c \ddot{u}\Big]\delta u \, dx \qquad (4)$$

$$+ \Big[- EI\frac{\partial^3 w}{\partial x^3} + EA_c\frac{\partial w}{\partial x}\left(\frac{\partial u}{\partial x} + \frac{1}{2}\left(\frac{\partial w}{\partial x}\right)^2\right)\Big]\delta w\Big|_o^{\ell} - V(\ell,t)\delta w(\ell,t) + \Big[EI\frac{\partial^2 w}{\partial x^2}\,\delta\frac{\partial w}{\partial x}\Big]\Big|_o^{\ell}$$

$$- M(\ell,t)\delta\frac{\partial w(\ell,t)}{\partial x} + \Big[EA_c\left(\frac{\partial u}{\partial x} + \frac{1}{2}\left(\frac{\partial w}{\partial x}\right)^2\right)\Big]\delta u\Big|_o^{\ell} - P(\ell,t)\delta u(\ell,t)\Big\}dt = 0 .$$

Since the variations δu and δw are arbitrary, equation (4) gives two coupled equations of motion

$$EI\frac{\partial^4 w}{\partial x^4} - \frac{\partial}{\partial x}\left(EA_c\frac{\partial w}{\partial x}\left(\frac{\partial u}{\partial x} + \frac{1}{2}\left(\frac{\partial w}{\partial x}\right)^2\right)\right) + \rho A_c\ddot{w} = 0 \qquad (5)$$

and

$$- \frac{\partial}{\partial x}\left(EA_c\left(\frac{\partial u}{\partial x} + \frac{1}{2}\left(\frac{\partial w}{\partial x}\right)^2\right)\right) + \rho A_c\,\ddot{u} = 0. \qquad (6)$$

The boundary conditions associated with equations (5) and (6) are

$$\Big[- EI\frac{\partial^3 w(\ell,t)}{\partial x^3} + EA_c\frac{\partial w(\ell,t)}{\partial x}\left(\frac{\partial u(\ell,t)}{\partial x} + \frac{1}{2}\left(\frac{\partial w(\ell,t)}{\partial x}\right)^2\right) - V(\ell,t)\Big]\delta w(\ell,t) = 0, \qquad (7)$$

$$\left[-EI\,\frac{\partial^3 w(0,t)}{\partial x^3} + EA_c\,\frac{\partial w(0,t)}{\partial x}\left(\frac{\partial u(0,t)}{\partial x} + \frac{1}{2}\left(\frac{\partial w(0,t)}{\partial x}\right)^2\right)\right]\delta w(0,t) = 0, \quad (8)$$

$$\left[EI\,\frac{\partial^2 w(\ell,t)}{\partial x^2} - M(\ell,t)\right]\delta\,\frac{\partial w(\ell,t)}{\partial x} = 0, \quad (9)$$

$$\left[EI\,\frac{\partial^2 w(0,t)}{\partial x^2}\right]\delta\,\frac{\partial w(0,t)}{\partial x} = 0, \quad (10)$$

$$\left[EA_c\left(\frac{\partial u(\ell,t)}{\partial x} + \frac{1}{2}\left(\frac{\partial w(\ell,t)}{\partial x}\right)^2\right) - P(\ell,t)\right]\delta u(\ell,t) = 0, \quad (11)$$

and

$$\left[EA_c\left(\frac{\partial u(0,t)}{\partial x} + \frac{1}{2}\left(\frac{\partial w(0,t)}{\partial x}\right)^2\right)\right]\delta u(0,t) = 0. \quad (12)$$

Since E, I, A_c, and ρ are constants, equations (5) and (6) reduce to

$$EI\,\frac{\partial^4 w}{\partial x^4} - EA_c\,\frac{\partial}{\partial x}\left(\frac{\partial w}{\partial x}\left(\frac{\partial u}{\partial x}\right)\right) + \rho A_c \ddot{w} = 0, \quad (13)$$

$$-E\,\frac{\partial^2 u}{\partial x^2} + \rho\ddot{u} = 0 \quad (14)$$

A possible form of solution to equations (13) and (14) is the straight configuration of the column,

$$u(x,t) = u_1(x,t), \quad (15)$$
$$w(x,t) = 0\ .$$

It is the stability of this form of solution that will be investigated.

Longitudinal Vibrations of a Column

Since the column is subjected to a longitudinal sinusoidal displacement at the end $x = 0$, it is necessary to investigate the effect of this displacement on the longitudinal vibrations. The uncoupled differential equation (14) for the longitudinal vibrations is

$$E \frac{\partial^2 u}{\partial x^2} - \rho \frac{\partial^2 u}{\partial t^2} = 0.$$

For a column excited by a longitudinal displacement $A_p \cos \Omega t$ at $x = 0$ and having a mass m at $x = \ell$, the boundary conditions, equations (11) and (12), become

$$u(0,t) = A_p \cos \Omega t \tag{16}$$

and

$$EA_c \frac{\partial u(\ell,t)}{\partial x} = - m \frac{\partial^2 u(\ell,t)}{\partial t^2} . \tag{17}$$

Assume a steady-state solution of the form

$$u(x,t) = \varphi(x) \cos \Omega t, \tag{18}$$

where the function $\varphi(x)$ is determined by applying the boundary conditions (16) and (17).

$$\varphi(x) = C_1 \sin ax + C_2 \cos ax$$

where

$$a = \sqrt{\frac{\rho\Omega^2}{E}} , \tag{19}$$

$$C_1 = \frac{EA_c A_p a \sin a\ell + m\Omega^2 A_p \cos a\ell}{EA_c a \cos a\ell - m\Omega^2 \sin a\ell} , \tag{20}$$

and

$$C_2 = A_p . \tag{21}$$

Therefore, the longitudinal displacement is given by

$$u(x,t) = (C_1 \sin ax + C_2 \cos ax) \cos \Omega t . \tag{22}$$

Reduction to the Rigid-Body Case

This analysis will consider a column and excitation system with the following approximate physical properties:

$$\begin{aligned} E &= 29 \cdot 10^6 \text{ psi} , \\ \rho &= 500 \text{ lb per cu ft} , \\ A_c &= .03 - .07 \text{ in}^2. , \\ \ell &= 16 - 36 \text{ in.} , \\ m &= 0.3 \text{ lb} . \end{aligned} \tag{23}$$

The maximum displacement and displacement frequency will be

$$A_p = .075 \text{ in.},$$
$$\Omega = 100 \text{ cycles per second}.$$

So,

$$a \simeq .004 \text{ per inch}$$
$$\cos(a\ell) \simeq 1 \quad \text{for} \quad 0 \leq x \leq \ell,$$
$$\sin(a\ell) \simeq 0 \quad \text{for} \quad 0 \leq x \leq \ell.$$

Substituting the physical properties (23) into equations (20) and (21) yields

$$C_1 \simeq 0,$$
$$C_2 = A_p.$$

The expression (22) for the longitudinal displacement now becomes simply

$$u(x,t) = A_p \cos \Omega t . \tag{24}$$

In other words, for systems having physical properties near those in expression (23), the first natural frequency of longitudinal vibration is much higher than the forcing frequency Ω. Therefore, the longitudinal displacement of the column can be considered a purely rigid-body motion as shown by equation (24).

An Equation for the Axial Force

The acceleration of any point on the rod is

$$\ddot{u}(x,t) = -A_p \Omega^2 \cos \Omega t .$$

By considering a compressive axial force as negative, the axial force at any cross section is

$$P(x,t) = (\rho A_c(\ell-x) + m)A_p \Omega^2 \cos \Omega t \ . \tag{25}$$

Transverse Free Vibrations of a Column

In the absence of an axial force, the differential equation of free transverse vibration of a column (5) reduces to

$$EI \frac{\partial^4 \Psi(x,t)}{\partial x^4} + \rho A_c \frac{\partial^2 \Psi(x,t)}{\partial t^2} = 0 \ , \tag{26}$$

where $\Psi(x,t)$ is the displacement in the z direction. Assume a solution to equation of the form

$$\Psi(x,t) = \psi n(x) e^{i\omega_n t} , \tag{27}$$

where ω_n is the nth natural frequency of transverse vibration. Substituting (27) into equation (26) yields

$$\frac{\partial^4 \psi n(x)}{\partial x^4} - \omega_n^2 \frac{\rho A_c}{EI} \psi_n(x) = 0 \ . \tag{28}$$

After letting

$$k^4 = \frac{\omega_n^2 \rho A_c}{EI}$$

and solving equation (28),

$$\psi_n(x) = A \cos kx + B \sin kx + C \cosh kx + D \sinh kx \ , \tag{29}$$

where A,B,C, and D are constants depending on the boundary conditions.

Boundary Conditions for Free Transverse Vibrations

For a column which is fixed at the end $x = 0$ and which has a mass m attached at the end $x = \ell$ the boundary conditions become

1) $\Psi(0,t) = 0$,

2) $\frac{\partial \Psi(0,t)}{\partial x} = 0$,

3) $V(\ell,t) = - m \frac{\partial^2 \Psi(\ell,t)}{\partial t^2} - me_c \frac{\partial^3 \Psi(\ell,t)}{\partial t^2 \partial x}$,

4) $V(\ell,t)e_c - M(\ell,t) = - J \frac{\partial \Psi^3(\ell,t)}{\partial x \partial t^2}$,

where $V(x,t)$ and $M(x,t)$ are the shear force and bending moment respectively on the column. From elementary beam theory in strength of materials,

$$EI \frac{\partial^2 \Psi(x,t)}{\partial x^2} = M(x,t)$$

and

$$EI \frac{\partial^3 \Psi(x,t)}{\partial x^3} = -V(x,t) .$$

The boundary conditions yield the following system of four homogeneous equations in the constants A, B, C, and D:

1) $A + C = 0,$ (30)

2) $B + D = 0,$ (31)

3) $[(me_c \omega_n^2 k - EIk^3)\sin k\ell - m\omega_n^2 \cos k\ell]A +$

$[(-me_c \omega_n^2 k + EIk^3)\cos k\ell - m\omega_n^2 \sin k\ell]B +$

$[(-me_c \omega_n^2 k - EIk^3)\sinh k\ell - m\omega_n^2 \cosh k\ell]C +$

$[(-me_c \omega_n^2 k - EIk^3)\cosh k\ell - m\omega_n^2 \sinh k\ell]D = 0 ,$ (32)

$$4)\quad [(J\omega_n^2 k - EIk^3 e_c)\sin k\ell + EIk^2 \cos k\ell]A +$$
$$[(-J\omega_n^2 k + EIk^3 e_c)\cos k\ell + EIk^2 \sin k\ell]B +$$
$$[(-J\omega_n^2 k - EIk^3 e_c)\sinh k\ell - EIk^2 \cosh k\ell]C +$$
$$[(-J\omega_n^2 k - EIk^3 e_c)\cosh k\ell - EIk^2 \sinh k\ell]D = 0 \qquad (33)$$

In order for this system of equations to have a non-trivial solution, the determinant of the coefficient matrix must vanish. For a given column, an iteration procedure must be used to determine the natural frequencies which make the determinant zero. Once the natural frequencies ω_1, ω_2, ..., ω_n have been found, the relative values between the constants A, B, C, and D are known, and the mode shape $\psi_n(x)$ is easily calculated for each ω_n. These mode shapes of free vibration will be used in Chapter III for the trial functions in the Galerkin analysis.

CHAPTER III

DERIVATION OF THE GOVERNING MATHIEU'S EQUATION

The problem now is to find the effect of the longitudinal displacement, equation (24), on the transverse motion of the column. Chapter II showed the derivation of the axial force $P(x,t)$ considering rigid-body longitudinal motion. If $P(x,t)$ is taken as

$$EA_c \frac{\partial u}{\partial x},$$

the uncoupled equation for transverse vibrations of a column (13) becomes

$$EI \frac{\partial^4 w}{\partial x^4} - \frac{\partial}{\partial x}\left(P(x,t) \frac{\partial w}{\partial x}\right) + \rho A_c \frac{\partial^2 w}{\partial t^2} = 0. \qquad (34)$$

A standard technique for solving equation (34) is Galerkin's method [14]. Let the differential operator L be defined by

$$L = EI \frac{\partial^4}{\partial x^4} - \frac{\partial}{\partial x}\left(P(x,t) \frac{\partial}{\partial x}\right) + \rho A_c \frac{\partial^2}{\partial t^2}.$$

If $w(x,t)$ is an exact solution to (34), then $L(w(x,t)) = 0$. Assume an approximate solution of the form

$$w_i(x,t) = \sum_{n=1}^{i} T_n(t)\ \theta_n(x),$$

where the $\theta_n(x)$ are functions satisfying the same boundary conditions as $w(x,t)$, and the $T_n(t)$ are undetermined functions. Then

$$L(w_i(x,t)) = \epsilon_i(x,t) \ ,$$

where $\epsilon_i(x,t)$ is an error function. If $w_i(x,t)$ is a satisfactory approximation to $w(x,t)$, then $\epsilon_i(x,t)$ is small. Galerkin's method imposes on the error function a set of orthogonality conditions

$$\int_o^\ell \epsilon_i(x,t)\ \theta_n(x)dx = 0 \ , \text{ or}$$

$$\int_o^\ell L(w_i(x,t))\ \theta_n(x)dx = 0, \qquad (n = 1,2,....,i). \tag{35}$$

Equation (35) yields a set of i equations

$$\int_o^\ell L\Big(\sum_{n=1}^{i} T_n(t)\ \theta_n(x)\Big)\ \theta_n(x)dx = 0, \qquad (n = 1,2,....,i) \ ,$$

for the determination of the functions $T_n(t)$ in the approximate solution of equation (34). The choice of $\theta_n(x)$ which satisfies the boundary conditions will be taken as $\psi_n(x)$, the modes of free vibration of a column derived in Chapter II.

Carrying out the indicated integrations would result in a system of i simultaneous Mathieu equations. These are very difficult to solve; so for simplicity, only a one-term series of the form

$$w_i(x,t) = \psi_n(x)\ T_n(t) \ ,$$

where n indicates the mode number, will be assumed. This is tantamount to saying that the column will exhibit transverse vibrations in one mode of free vibration only and that there will be no coupling effects between

the various modes. The experimental part will serve to test the validity of the one-term Galerkin analysis with the free vibration mode shape.

The one-term Galerkin method yields

$$\int_0^{\ell} \left\{ EI \frac{\partial^4 (\psi_n(x)\, T_n(t))}{\partial x^4} - \frac{\partial}{\partial x}\left[P(x,t) \frac{\partial (\psi_n(x)\, T_n(t))}{\partial x} \right] \right.$$

$$\left. + \rho A_c \frac{\partial^2}{\partial t^2} (\psi_n(x)\, T_n(t)) \right\} \psi_n(x)\, dx = 0,$$

where

$$P(x,t) = [(\ell - x)\rho A_c + m]\Omega^2 A_p \cos \Omega t,$$

$$\psi_n(x) = A \cos kx + B \sin kx + C \cosh kx + D \sinh kx,$$

and

$$k = \left[\omega_n^2 \frac{\rho A_c}{EI} \right]^{\frac{1}{4}}.$$

The above integral is broken into three parts, and the indicated integration is carried out on each.

$$\int_0^{\ell} EI \frac{\partial^4}{\partial x^4} (\psi_n(x)\, T_n(t))\, \psi_n(x) dx =$$

$$EI\, k^4 \left\{ \frac{(A^2+B^2)}{2} x + \frac{(C^2-D^2)}{2} x + \frac{(A^2-B^2)}{4K} \sin 2kx + \frac{(C^2+D^2)}{4k} \sinh 2kx \right.$$

$$+ \frac{AB}{k} \sin^2 kx + \frac{CD}{k} \sinh^2 kx + \frac{AC}{k} [\sinh kx \cos kx + \cosh kx \sin kx]$$

$$\left. + \frac{AD}{k} [\cosh kx \cos kx + \sinh kx \sin kx] \right.$$

$$+\frac{BC}{k}[\sinh kx \sin kx - \cosh kx \cos kx]$$

$$+\frac{BD}{k}[\cosh kx \sin kx - \sinh kx \cos kx]\Big\}\Big|_{o}^{\ell} T_n(t) = \beta T_n(t).$$

$$\int_o^{\ell} \rho A_c \frac{\partial^2}{\partial t^2}(\psi_n(x)\, T_n(t))\, \psi_n(x)dx =$$

$$\rho A_c\Big\{\frac{(A^2+B^2)}{2}x + \frac{(C^2-D^2)}{2}x + \frac{(A^2-B^2)}{4k}\sin 2kx$$

$$+\frac{(C^2+D^2)}{4k}\sinh 2kx + \frac{AB}{k}\sin^2 kx + \frac{CD}{k}\sinh^2 kx$$

$$+\frac{AC}{k}[\sinh kx \cos kx + \cosh kx \sin kx]$$

$$+\frac{AD}{k}[\cosh kx \cos kx + \sinh kx \sin kx]$$

$$+\frac{BC}{k}[\sinh kx \sin kx - \cosh kx \cos kx]$$

$$+\frac{BD}{k}[\cosh kx \sin kx - \sinh kx \cos kx]\Big\}\Big|_{o}^{\ell} \frac{d^2Tn(t)}{dt^2} = \alpha \frac{d^2Tn(t)}{dt^2}\ .$$

The third integral is

$$-\int_o^{\ell} \frac{\partial}{\partial x}\Big[P(x,t)\,\frac{\partial}{\partial x}(\psi_n(t)T_n(t))\Big]\,\psi_n(x)dx. \qquad (36)$$

when integrated by parts, expression (36) becomes

$$-T_n(t)\Big\{P(x,t)\psi_n(x)\,\frac{\partial}{\partial x}(\psi_n(x))\Big|_o^{\ell} - \int_o^{\ell} P(x,t)\Big(\frac{\partial(\psi_n(x))}{\partial x}\Big)^2\,dx\Big\} \qquad (37)$$

After making the substitutions that

$$KK1 = m + \ell\rho A_c$$

and

$$KK2 = -\rho A_c \ ,$$

the equation for the axial force becomes

$$P(x,t) = (KK1 + KK2\ x)\Omega^2 A_\rho \cos \Omega t.$$

Now expression (37) reduces to

$$- \Big\{(KK1 + KK2\ x)(A \cos kx + B \sin kx + C \cosh kx + D \sinh kx)$$

$$(-A \sin kx + B \cos kx + C \sinh kx + D \cosh kx)k\Big|_0^{\ell} - k^2\Big\{KK1\Big[\frac{(A^2+B^2)}{2}x$$

$$+ \frac{(D^2-C^2)}{2}x + \frac{(B^2-A^2)}{4k} \sin 2kx + \frac{(C^2+D^2)}{4k}\sinh 2kx - \frac{AB}{k} \sin^2 kx$$

$$+ \frac{CD}{k} \sinh^2 kx + \frac{AC}{k}[\sinh kx \cos kx - \cosh kx \sin kx]$$

$$+ \frac{AD}{k}[\cosh kx \cos kx - \sinh kx \sin kx]$$

$$+ \frac{BC}{k}[\sinh kx \sin kx + \cosh kx \cos kx]$$

$$+ \frac{BD}{k}[\cosh kx \sin kx + \sinh kx \cos kx]\Big] + KK2\Big[\frac{(A^2+B^2)}{4}x^2 + \frac{(D^2-C^2)}{4}x^2$$

$$+ \frac{(B^2-A^2)}{2}\Big(\frac{\cos 2kx + 2kx \sin 2kx}{(2k)^2}\Big)$$

$$+ \frac{(C^2+D^2)}{2}\Big(\frac{2kx \sinh 2kx - \cosh 2kx}{(2k)^2}\Big) - AB\Big(\frac{\sin 2kx - 2kx \cos 2kx}{(2k)^2}\Big)$$

$$+ CD\left(\frac{2kx\cosh 2kx - \sinh 2kx}{(2k)^2}\right)$$

$$- A(C+D)\left(xe^{kx}\frac{\sin kx - \cos kx}{2k} + \frac{e^{kx}\cos kx}{2k^2}\right)$$

$$+ B(C+D)\left(xe^{kx}\frac{\cos kx + \sin kx}{2k} - \frac{e^{kx}\sin kx}{2k^2}\right)$$

$$- A(D-C)\left(xe^{-kx}\frac{-\sin kx - \cos kx}{2k} - \frac{e^{-kx}\cos kx}{2k^2}\right)$$

$$+ B(D-C)\left(xe^{-kx}\frac{-\cos kx + \sin kx}{2k} + \frac{e^{-kx}\sin kx}{2k^2}\right)\Bigg]\Bigg\}\Bigg|_0^{\ell}\Omega^2 A_p\cos\Omega t\cdot T_n(t)$$

$$= \gamma\,\Omega^2 Ap\,\cos\Omega t\;T_n(t).$$

The Galerkin analysis yields a Mathieu's equation

$$\alpha\frac{d^2Tn(t)}{dt^2} + (\beta + \gamma\Omega^2 Ap\,\cos\Omega t)\,Tn(t) = 0,$$

where α, β, and γ are constants determined by the previous integrations.

CHAPTER IV

ANALYTICAL DETERMINATION OF THE INSTABILITY REGIONS

From Chapter III, Galerkin's method yields the Mathieu's equation

$$\alpha \frac{d^2Tn(t)}{dt^2} + (\beta + \gamma\Omega^2 A_p \cos \Omega t)Tn(t) = 0 . \tag{38}$$

Dividing equation (38) by α gives

$$\frac{d^2Tn(t)}{dt^2} + (\omega_n^2 + \bar{c}\Omega^2 A_p \cos \Omega t)Tn(t) = 0, \tag{39}$$

where

$$\frac{\beta}{\alpha} = \omega_n^2 \quad \text{and} \quad \bar{c} = \frac{\gamma}{\alpha}.$$

Equation (39) will have stable solutions i.e., the solutions $T_n(t)$ will remain bounded for all time t, if certain relationships hold between the coefficients ω_n^2 and $\bar{c}\Omega^2 A_p$. Bolotin [9] demonstrated that the regions of unboundedly increasing solutions are separated from the regions of stability by periodic solutions with periods $\frac{2\pi}{\Omega}$ and $\frac{4\pi}{\Omega}$. More exactly, solutions or identical periods bound the regions of instability, and two solutions of different periods bound the regions of stability.

McLachlan [7] gives the canonical form of Mathieu's equation as

$$\frac{d^2Y(z)}{dz^2} + (a - 2q \cos 2z)Y(z) = 0. \tag{40}$$

After making the change of variable $2z = \Omega t$, equation (39) becomes

$$\frac{\Omega^2}{4}\frac{d^2Tn(z)}{dz^2} + (\omega_n^2 + \bar{c}\Omega^2 A_p \cos 2z)Tn(z) = 0. \qquad (41)$$

Letting

$$a = \frac{4\omega_n^2}{\Omega^2} \quad \text{and} \quad q = -2\bar{c}\,Ap\ ,$$

equation (41) is put in the canonical form of (40). The stability boundaries to equation (40) can be determined by representing the coefficient a in terms of a converging power series of q[7].* The principal instability region is bounded by the following two equations:

$$a = b_1 = 1 - q - \frac{q^2}{8} + \frac{q^3}{64} - \frac{q^4}{1536} - \frac{11}{38863}q^5$$

$$+ \frac{49}{589824}q^6 - \frac{55}{9437184}q^7 - \frac{265}{113246208}q^8 + O(q^9)\ ,$$

$$a = a_1 = 1 + q - \frac{q^2}{8} - \frac{q^3}{64} - \frac{q^4}{1536} + \frac{11}{38863}q^5$$

$$+ \frac{49}{589824}q^6 + \frac{55}{9437184}q^7 - \frac{265}{113246208}q^8 + O(q^9)\ ,$$

where $O(\ )$ represents the higher order terms in the series. Other power series for the higher regions of instability are given in [7].

Since

$$a = \frac{4\omega_n^2}{\Omega^2} \quad \text{and} \quad q = -2\bar{c}Ap\ ,$$

stability charts of Ω versus A_p can be plotted. Of course, each chart is

*pp. 11-17.

for a particular mode shape $\psi_n(x)$ of free vibration and set of physical constants for the column. The only variables in Mathieu's equation are the base amplitude A_p and the displacement frequency Ω.

Influence of Damping on the Instability Regions

If the column is subjected to a viscous damping force, equation (39) becomes

$$\frac{d^2Tn(t)}{dt^2} + 2\epsilon_n \frac{dTn(t)}{dt} + (\omega_n^2 + \bar{c}\Omega^2 Ap \cos \Omega t)Tn(t) = 0, \qquad (42)$$

where ϵ_n is the coefficient of damping. For a Mathieu's equation in the form of (42), instability regions are difficult to obtain by using a power series expansion as in the previous section. Bolotin [9] used a different technique. Since the stability regions are separated from the instability regions by solutions of periods $\frac{2\pi}{\Omega}$ and $\frac{4\pi}{\Omega}$, assume a solution of period $\frac{2\pi}{\Omega}$ of the form

$$Tn(t) = b_o + \sum_{j=2,4,6}^{\infty} \left(a_j \sin \frac{j\Omega t}{2} + b_j \cos \frac{j\Omega t}{2}\right) \qquad (43)$$

and of period $\frac{4\pi}{\Omega}$ of the form

$$Tn(t) = \sum_{j=1,3,5}^{\infty} \left(a_j \sin \frac{j\Omega t}{2} + b_j \cos \frac{j\Omega t}{2}\right) \qquad (44)$$

By letting $\bar{c}\Omega^2 A_p = -2\mu\omega_n^2$, equation (42) can be put into the form*

$$\frac{d^2Tn(t)}{dt^2} + 2\epsilon_n \frac{dTn(t)}{dt} + \omega_n^2(1-2\mu \cos \Omega t)Tn(t) = 0. \qquad (45)$$

*See Bolotin [9] p. 33.

If equations (43) and (44) are substituted into (45), two systems of homogeneous equations in a_j and b_j result. The requirement that the determinant of the coefficient matrix vanish, to yield non-trivial solutions of a_j and b_j, gives the instability boundaries. This algebraic process is given in [9]*, and the approximate instability boundaries are derived. If $\Delta_n = \frac{2\pi\epsilon_n}{\omega_n}$, and Ω_{*1}, Ω_{*2}, and Ω_{*3} denote the forcing frequencies for the first, second, and third instability regions respectively, then Bolotin gives

$$\Omega_{*1} = 2\omega_n\sqrt{1 \pm \sqrt{\mu^2 - \left(\frac{\Delta n}{\pi}\right)^2}},$$

$$\Omega_{*2} = \omega_n\sqrt{1 - \mu^2 \pm \sqrt{\mu^4 - \left(\frac{\Delta n}{\pi}\right)^2 (1-\mu^2)}}, \qquad (46)$$

$$\Omega_{*3} = \frac{2}{3}\,\omega_n\sqrt{1-\xi},$$

where

$$\xi = \frac{\frac{8}{9}\,\mu^2 \pm \sqrt{\mu^6 - \left(\frac{\Delta n}{\pi}\right)^2\left[\frac{64}{81} - \frac{2}{3}\,\mu^2\right]}}{\frac{64}{81} - \mu^2}.$$

It should be noted that the above equations were derived assuming $\mu \leq 0.3$ and $\Delta_n \leq 0.05$. The values for μ and Δ_n in this thesis are well below these limits.

*pp. 33-39.

CHAPTER V

THE EXPERIMENTAL PROCEDURE

Experimental Apparatus

The experimental apparatus is shown in Figure 2. A thin rectangular column was mounted vertically on the table of a 25 lb. vibration fatigue testing machine which had independent amplitude and frequency control. The testing machine used in this experiment had an amplitude range of 0-.075 inches and a frequency range of 0-100 cycles per second. Two rectangular blocks bolted to the table provided a vise grip to insure the column had a cantilever support at its base. A strain gage was attached near the column's base to measure the amount of damping present in each mode. An accelerometer was mounted on the table to monitor its motion, and if the motion was erratic, the vibration machine was adjusted to make the waveform closer to sinusoidal. The maximum table acceleration could have been read directly from the accelerometer, but unfortunately, the calibration was inaccurate. Instead, the base acceleration was calculated by measuring the base amplitude with a micrometer and the base frequency with a strobotac light. The signals from both the strain gage and the accelerometer were fed through amplifiers to separate beams of a Tektronic 502A dual-beam oscilloscope. This allowed simultaneous observation of both the strain and table waveform outputs. See Figures 12-14.

Measurement of Damping

In Chapter IV equation (42) resulted when a viscous damping force

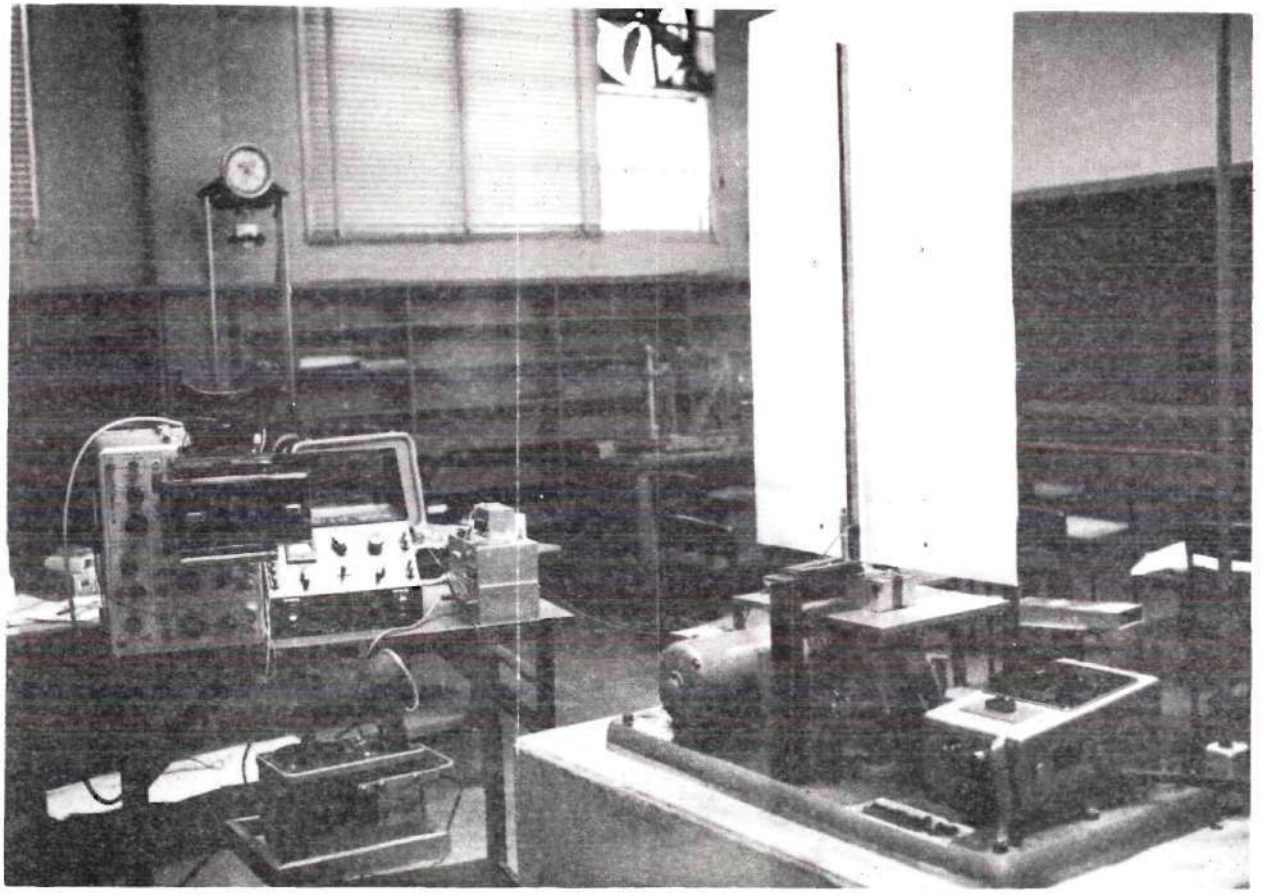

Figure 2. The Experimental Apparatus.

was included in the analysis. The logarithmic decrement for the nth mode was defined to be $\Delta_n = \frac{2\pi\epsilon_n}{\omega_n}$. This decrement can be expressed as

$$\Delta_n = \frac{1}{j} \frac{Tn(t)}{Tn(t + jP)} ,$$

where j is an integer and P is the period of damped vibration. Since the longitudinal strains $\bar{\epsilon}_{Ln}$ are proportional to the lateral deflections,

$$\frac{Tn(t)}{Tn(t + jP)} = \frac{\bar{\epsilon}_{Ln}(t)}{\bar{\epsilon}_{Ln}(t + jP)} .$$

Therefore, a measurement of the magnitudes of the longitudinal strains between periods of damped vibration will give Δ_n. To calculate the damping in the first mode, the column was simply plucked at one end and allowed to vibrate freely. A time exposed photograph was taken of the strain trace for one sweep across the oscilloscope screen. To determine the damping in the higher modes, the column was made unstable in the desired mode, and the base displacement was quickly stopped. Again a time photograph was taken of the strain trace of the damped motion.

It should be noted that the determination of the logarithmic decrement became more difficult as the mode number increased. There are two reasons for this. When the column became unstable in one of the higher modes and the vibration machine was quickly stopped, oscillations occurred not only in this mode but in the lower modes as well. Also in the higher modes, the column damping was not entirely viscous, and the decrement decreased as the magnitude of the strain decreased. Figures 15 - 19

show the strain oscilloscope trace for various columns and mode shapes.

Experimental Determination of the Instability Regions

Since the analytical determination of the instability regions was based on the stability of the straight configuration, the same criterion must be applied for the experimental analysis. The purpose of the experimental work was to determine the corresponding values of the variables Ω and A_p when the straight column began exhibiting lateral vibrations.

After the table amplitude had been set to its maximum value on the vibration machine, the displacement frequency was slowly increased from zero. As the frequency increased, small perturbations were given to the center of the column. At a certain frequency the column exhibited large transverse vibrations. This point constituted the lower bound of the instability region. The frequency was again increased until the straight configuration of the column became stable and then decreased to the point of instability which gave the upper boundary of the instability region. Several runs were made for each amplitude setting, and the frequency of the base and the base amplitude were recorded for each run. The table displacement was reduced about .01 inches, and the procedure repeated. It was observed that the table displacement could be reduced to a point where no lateral vibrations were observed. This was caused by the effect of damping cutting off part of the instability region.

CHAPTER VI

RESULTS AND CONCLUSIONS

Chapters II-IV showed the analytical determination of the instability boundaries of the straight configuration of a cantilever column with a sinusoidal longitudinal end displacement. The derivation of the governing Mathieu equation was based upon a one-term Galerkin analysis using the free vibration mode shape. The numerical results of the analytical part, with and without the effect of viscous damping, is given in Appendix II.

Chapter V gave the procedure for experimentally determining the principal instability regions and for calculating the damping in each mode. Experimental results are given in Appendix I. Figures 3-5 show plots of the principal instability regions for both analytical and experimental results. There is a slight shift upwards in the experimental region probably caused by using too low a value for the natural frequency ω_n. Nevertheless, the agreement between theory and experiment is excellent, and it can be concluded that a one-term Galerkin analysis is sufficiently valid for the physical system considered in the experiment.

The Effect of Damping

Damping contributes an important effect to the instability regions, particularly for the first mode of vibration and for the higher regions of instability. Figure 6 shows that damping causes the higher regions of instability to lie farther from the $\frac{\Omega}{2\omega_n}$ axis. The second region of

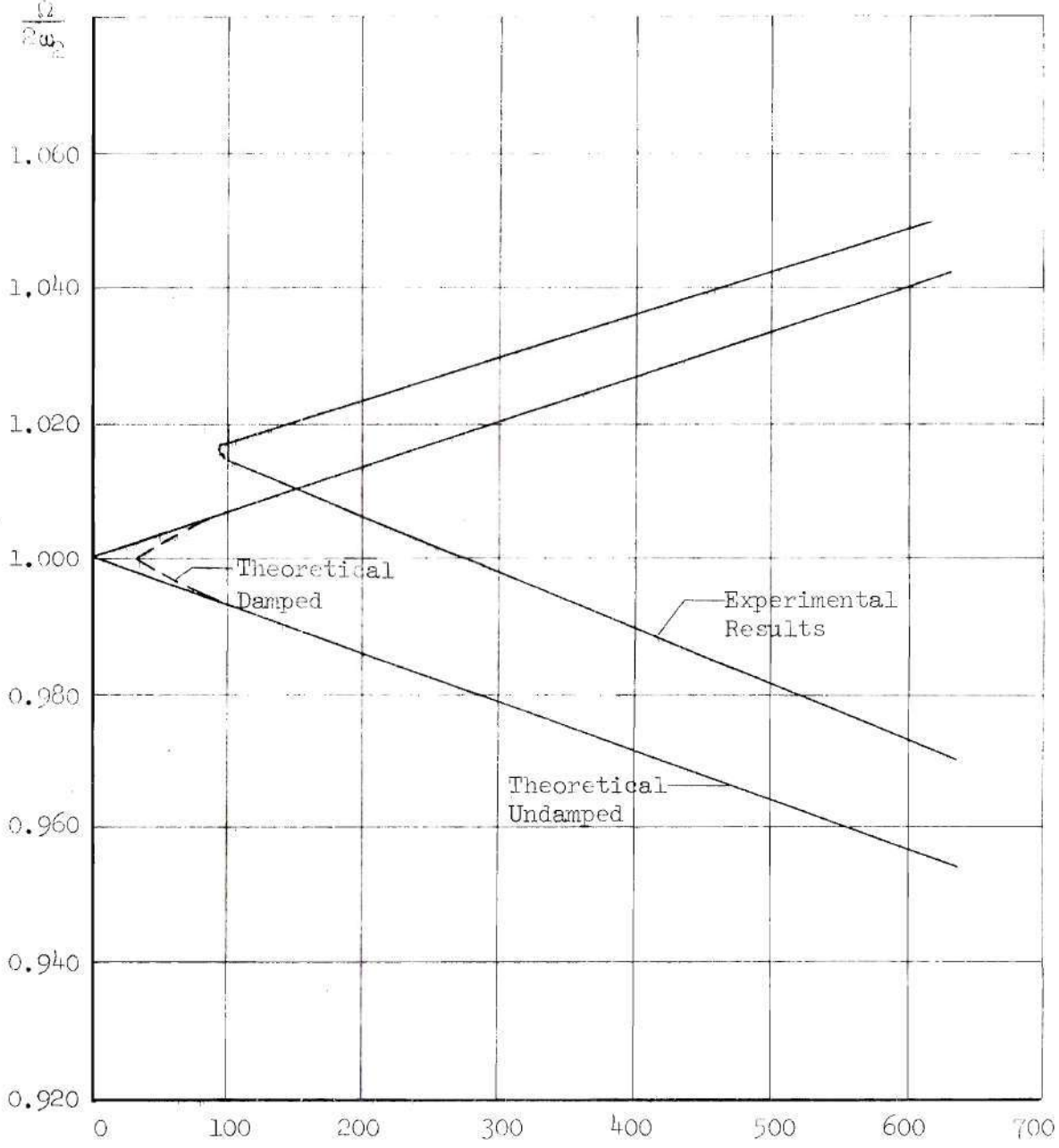

Figure 3. Analytical and Experimental Principal Instability Region for Second Mode Vibration.

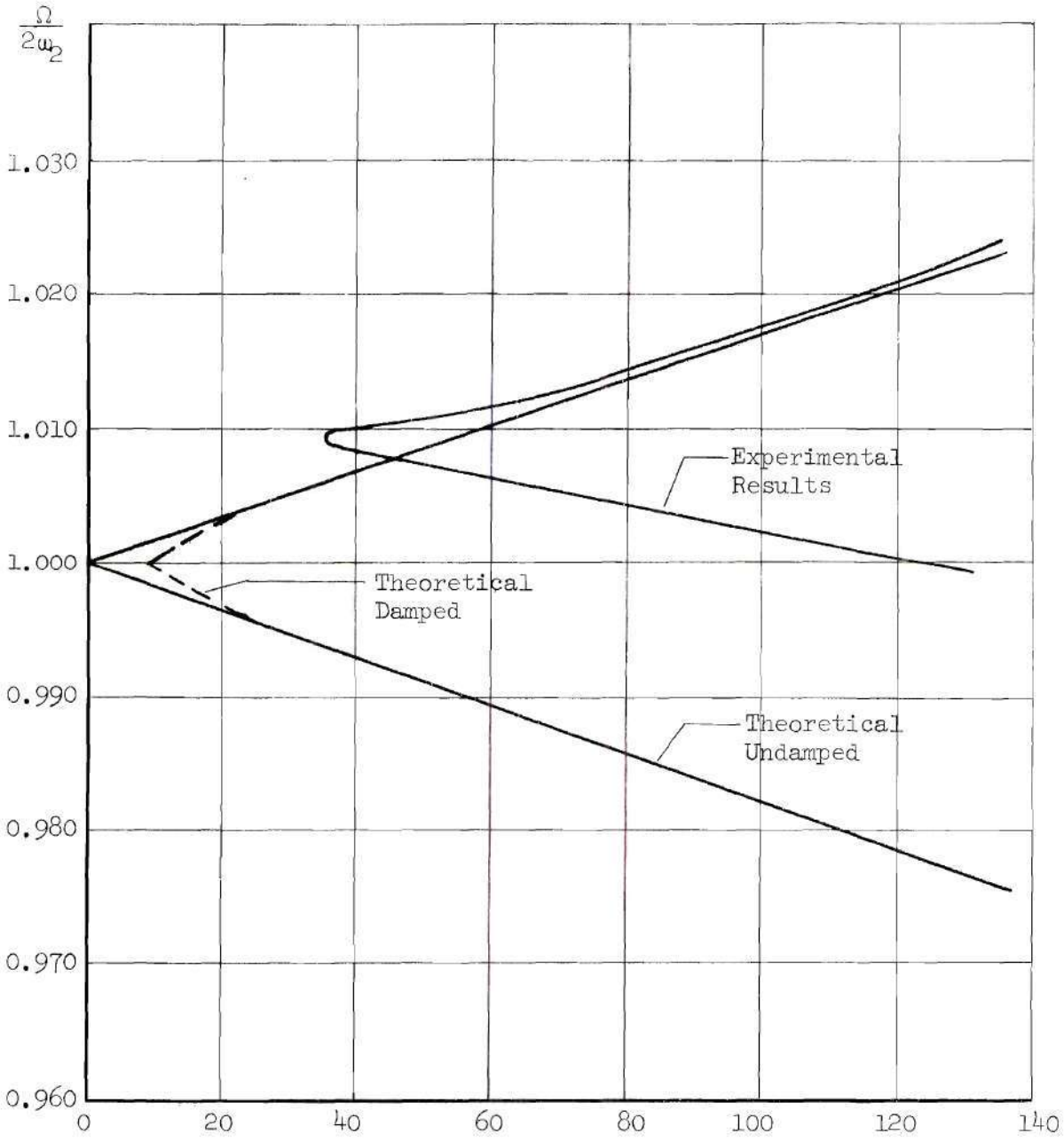

Figure 4. Analytical and Experimental Principal Instability Region for Second Mode Vibration.

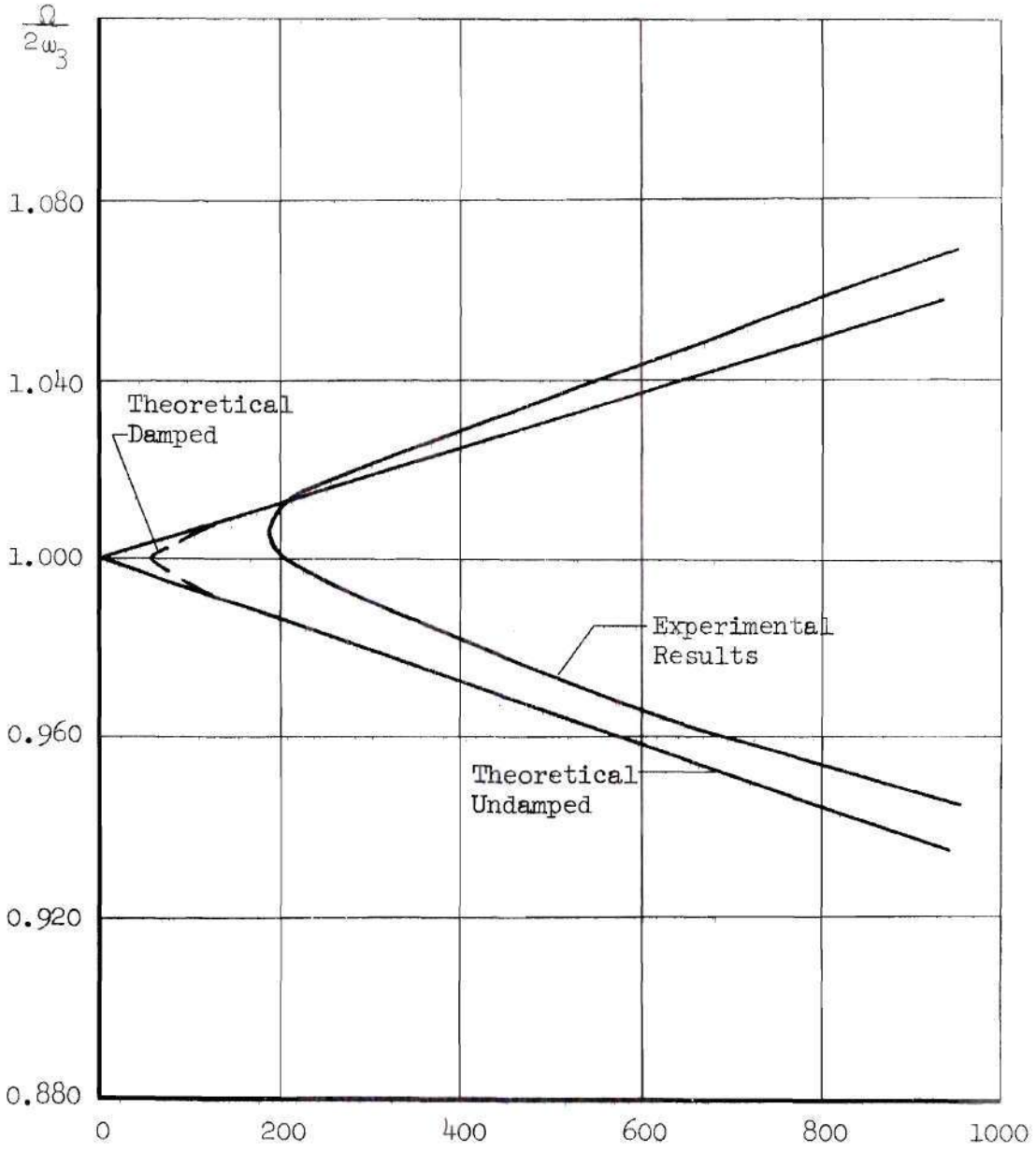

ℓ = 34.813 in. $\quad \Delta_3 = 0.006$

d = 1.00 in. $\quad \omega_3 = 29.0$ cycles per second

h = 0.0625 in.

Figure 5. Analytical and Experimental Principal Instability Region for Third Mode Vibration.

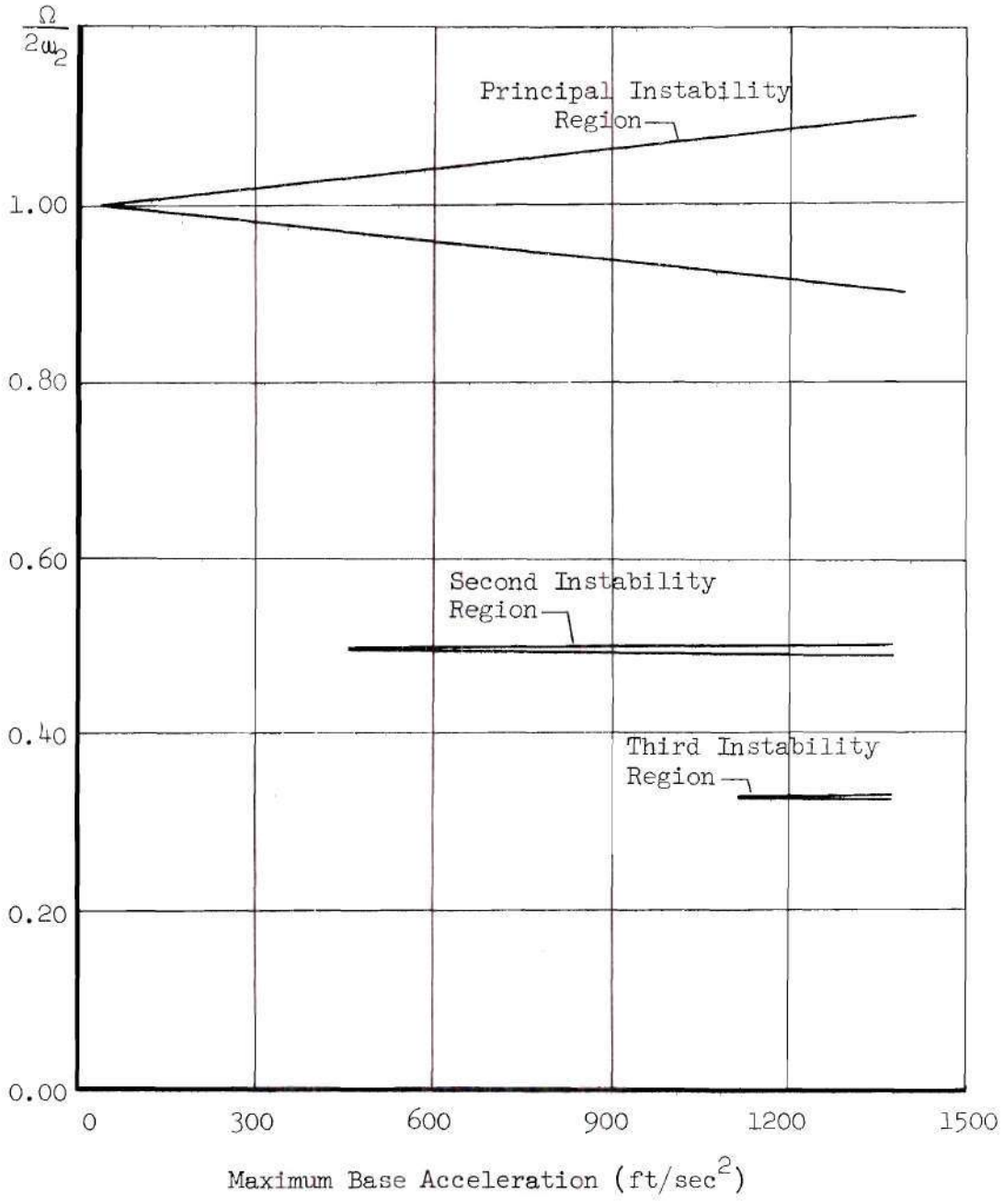

ℓ = 16.219 in. $\quad\quad$ Δ_2 = 0.013

d = 1.250 in. $\quad\quad$ ω_2 = 24.0 cycles per second

h = 0.03125 in.

Figure 6. The Influence of Damping on the First Three Analytical Regions of Instability.

instability was observed experimentally, but the upper and lower boundaries could not be accurately determined because the region become so narrow.

The effect of damping also explains why first mode instability was not observed. The maximum table acceleration is

$$A_{max} = A_p \Omega^2 . \tag{47}$$

Taking the square root of (47) and dividing by $2\omega_n$ yields

$$\frac{\Omega}{2\omega_n} = \sqrt{A_{max.}} \Big/ (2\omega_n \sqrt{A_p}) .$$

Since ω_n and A_p are constants for a given mode and table amplitude, equation is a parabola in $\frac{\Omega}{2\omega_n}$ and A_{max}. Figure 7 shows that the line of maximum table amplitude, A_p = .0750 in., does not cross the theoretical damped instability region. Therefore, first mode instability is not expected. If the table amplitude could have been increased, instability would have occurred.

Discussion of Farrell's [13] Results

In 1965 Farrell studied, both analytically and experimentally, the problem presented in this thesis. Instead of using a Galerkin analysis to determine the Mathieu equation, he took the value of the axial force $P(x,t)$ at $x = \frac{\ell}{2}$ and considered this force constant along the column. If it is assumed that the unstable configuration is the same as the modes of free vibration, the resulting Mathieu equation is

$$\frac{d^2 T_n(t)}{dt^2} + (\omega_n^2 \pm \frac{\ell}{2} k^2 A_p \Omega^2 \cos \Omega t) T_n(t) = 0 .$$

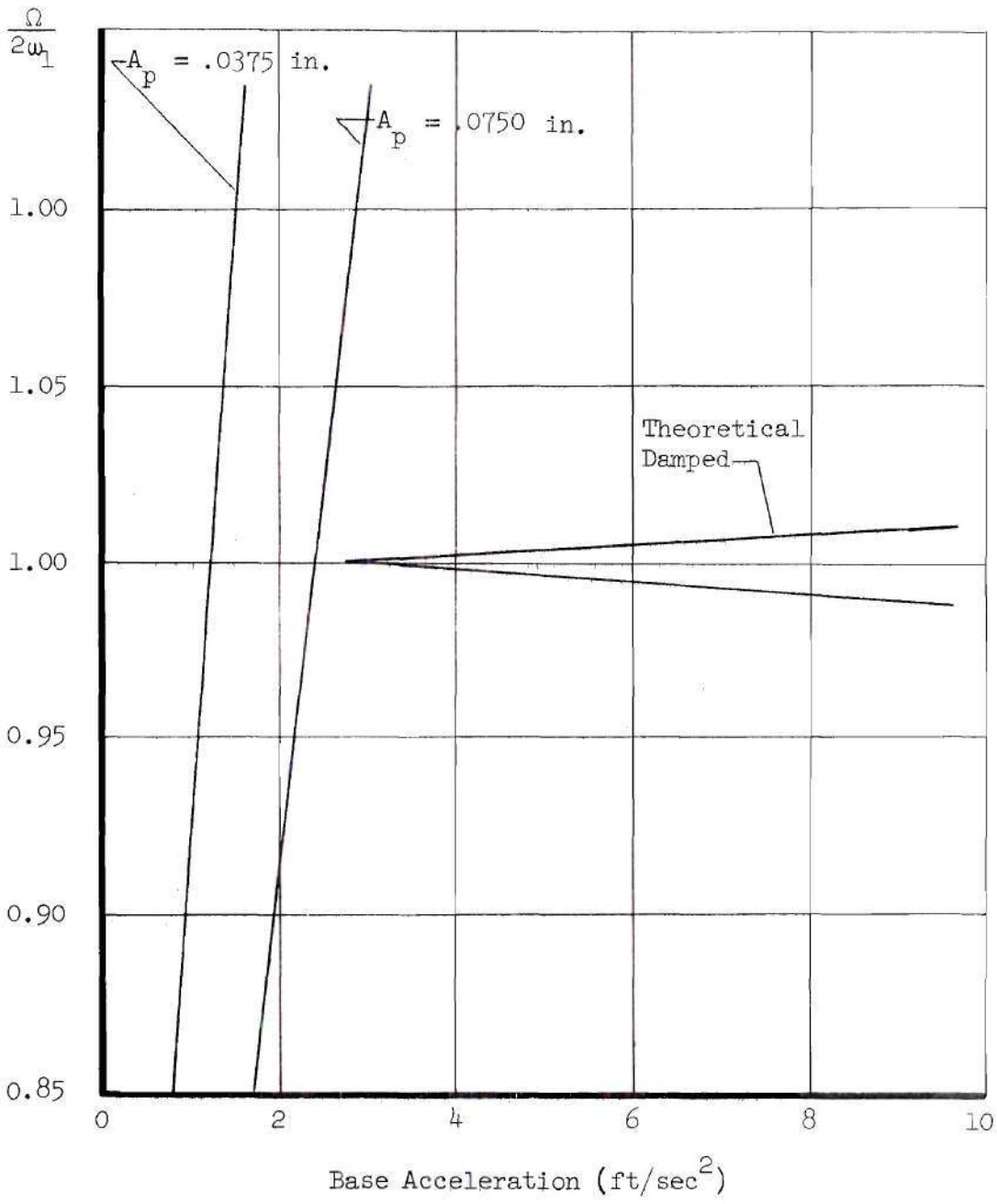

ℓ = 34.81 in.

d = 1.00 in.

h = 0.0625 in.

Δ_1 = 0.022

ω_1 = 1.56 cycles per second

Figure 7. Lines of Constant Amplitude Plotted on the First Mode Principal Instability Region.

Equation (39) in Chapter IV gave the Mathieu equation as

$$\frac{d^2 T_n(t)}{dt^2} + (\omega_n^2 + \bar{c}\, A_p\, \Omega^2 \cos \Omega t) T_n(t) = 0 ,$$

where $\bar{c}$ is a constant determined from the Galerkin analysis. These two equations agree identically if $\bar{c} = \frac{\ell}{2} k^2$. Sample calculations yield $\bar{c} < k^2 \frac{\ell}{2}$ and the percentage difference in $\bar{c}$ and $k^2 \frac{\ell}{2}$ increases for higher mode numbers.

In terms of the stability charts, values of $\bar{c} < k^2 \frac{\ell}{2}$ mean the regions of instability as derived in this paper are narrower than those plotted by Farrell. Figures 8 and 9 show this shift and seem to indicate the one-term Galerkin analysis yields instability regions closer to the experimental than by considering the axial force at $\frac{\ell}{2}$ constant along the column. Farrell's experimental region also fell inside his analytical.

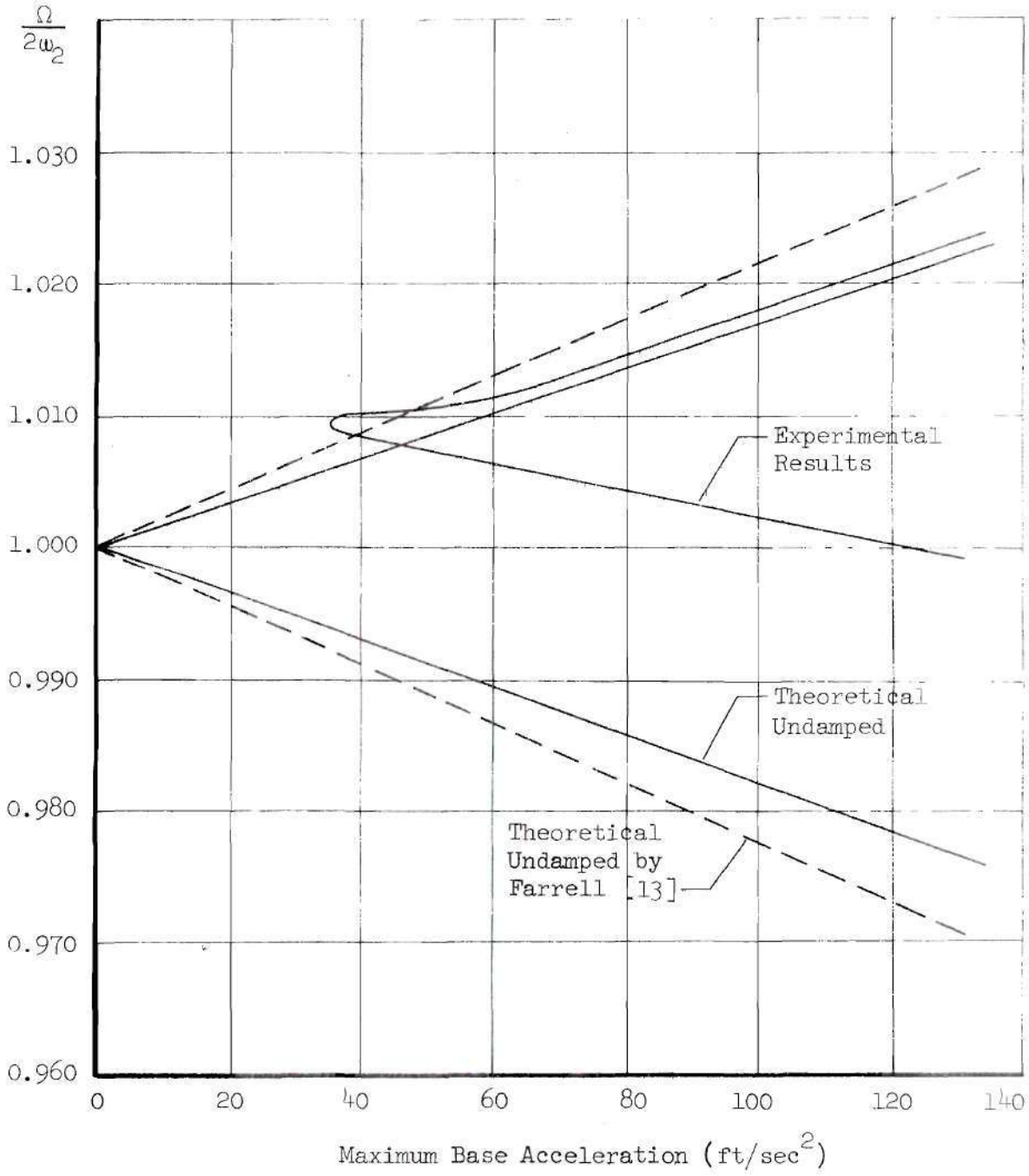

ℓ = 34.813 in. Δ_2 = 0.010

d = 1.00 in. ω_2 = 10.4 cycles per second

h = 0.0625 in.

Figure 8. Comparison to Farrell's Theoretical Undamped Principal Instability Region.

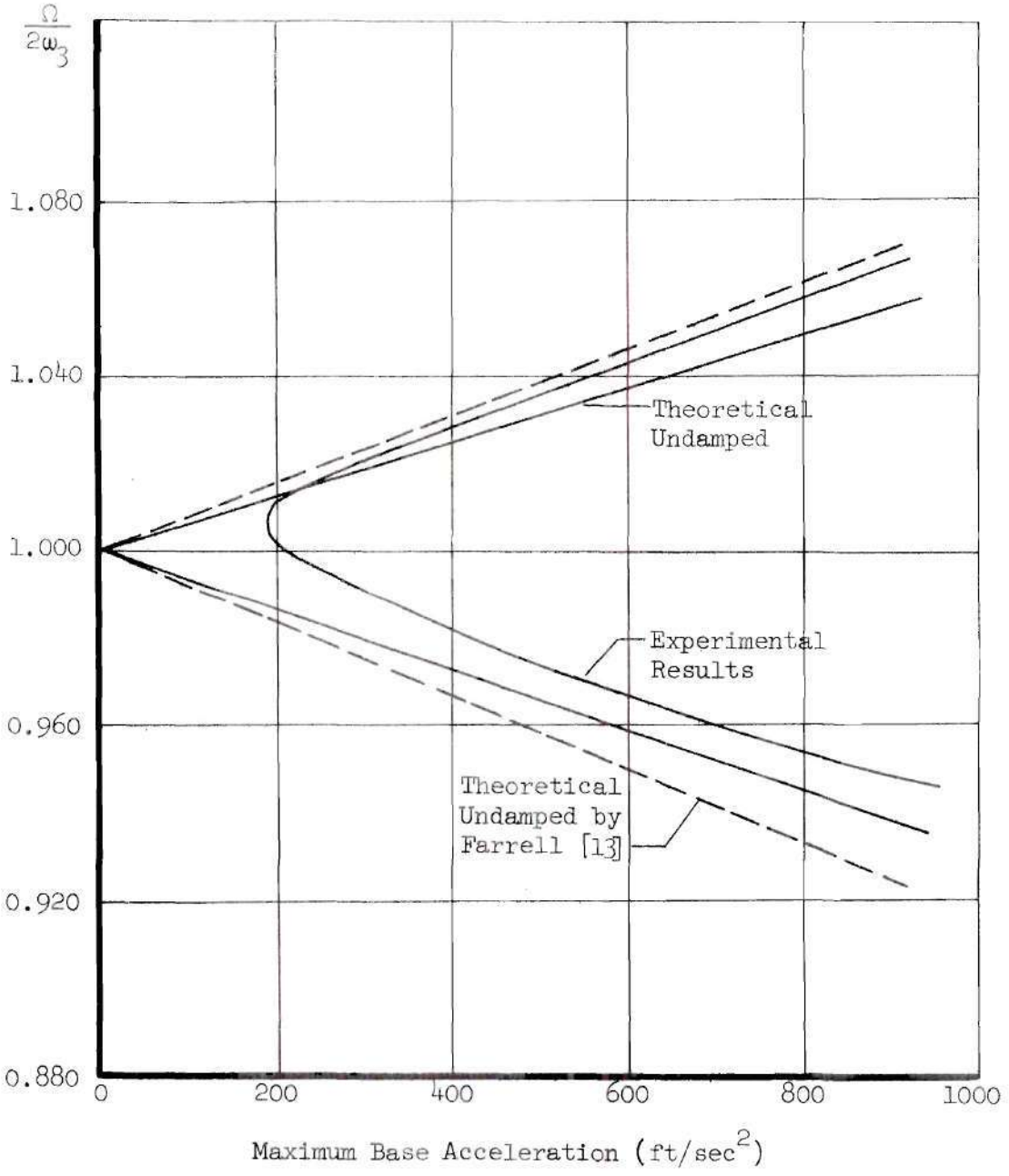

ℓ = 34.813 in. $\quad\quad$ Δ_3 = 0.006

d = 1.00 in. $\quad\quad$ ω_3 = 29.0 cycles per second

h = 0.0625 in.

Figure 9. Comparison to Farrell's Theoretical Undamped Principal Instability Region.

APPENDIX I

EXPERIMENTAL OBSERVATIONS AND CALCULATIONS

Figures 10 and 11 show the unstable second and third mode configurations respectively of a column specimen. Figures 12-14 show the relationship between the bending strain and the base displacement in these unstable states. The decrements of damping Δ_n were calculated from Figures 15-19. Tables 1-3 give the data collected to determine the experimental principal instability regions plotted in Figures 3-5.

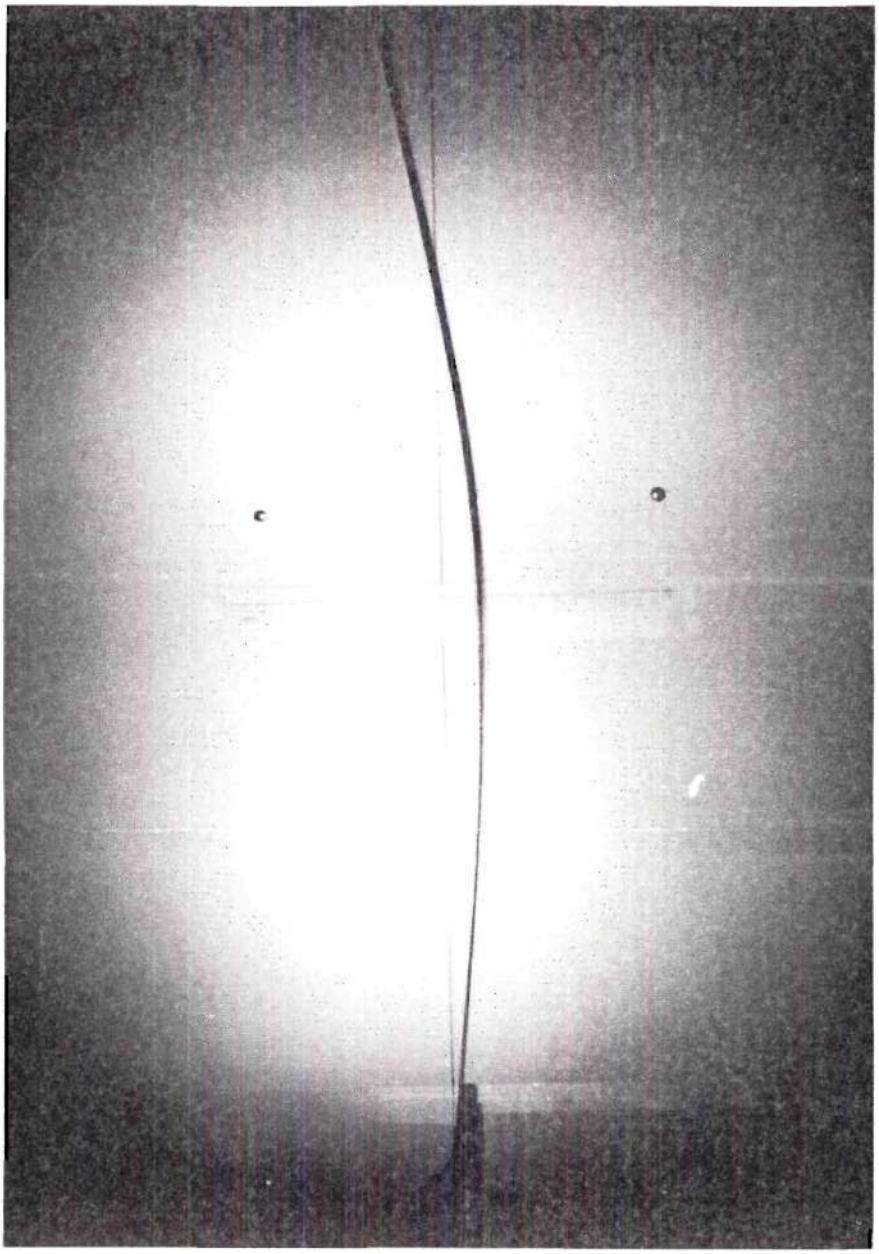

ℓ = 34.813 in. h = 0.0625 in.

d = 1.00 in. ω_2 = 10.4 cycles per second

Figure 10. Second Mode Unstable Configuration.

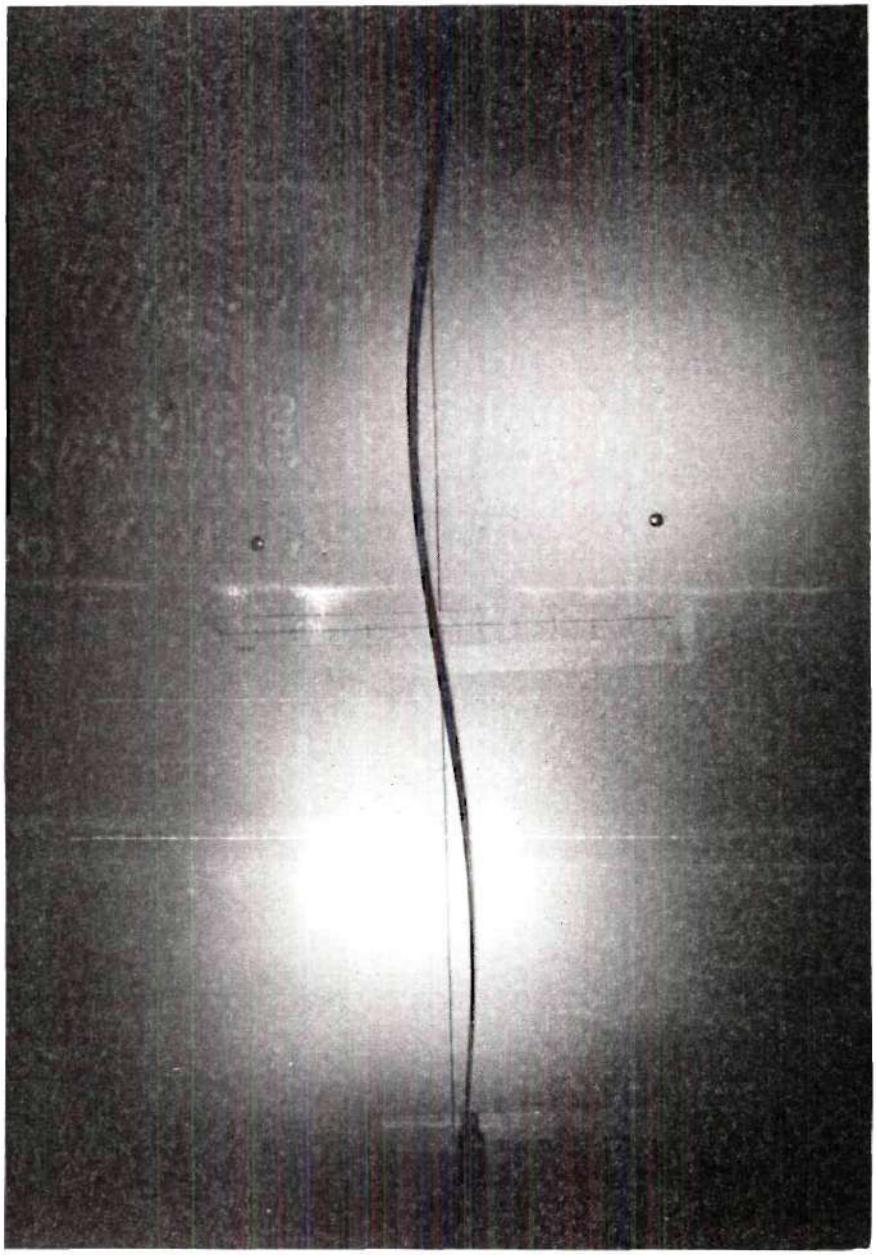

ℓ = 34.813 in. h = 0.0625 in.

d = 1.00 in. ω_3 = 29.0 cycles per second

Figure 11. Third Mode Unstable Configuration.

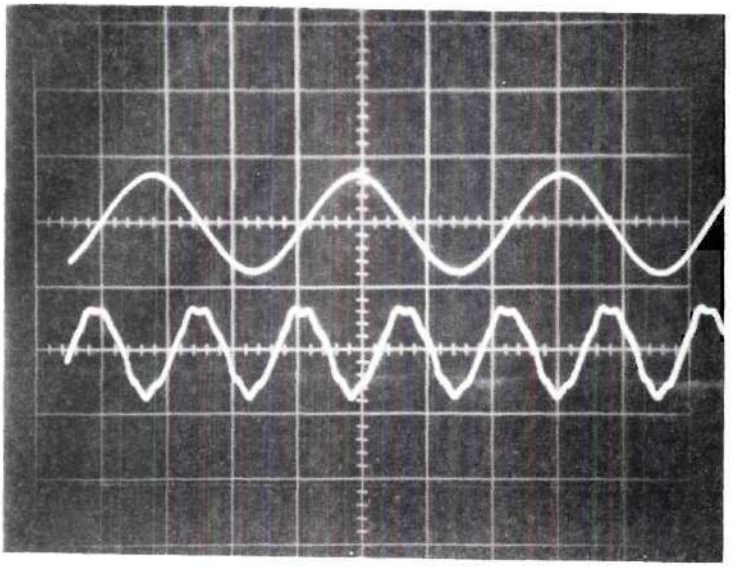

ℓ = 16.219 in. ω_2 = 24.0 cycles per second

d = 1.25 in.

h = 0.03125 in.

Figure 12. The Relationship between the Bending Strain (Top) and the Base Displacement (Bottom) for Second Mode Instability.

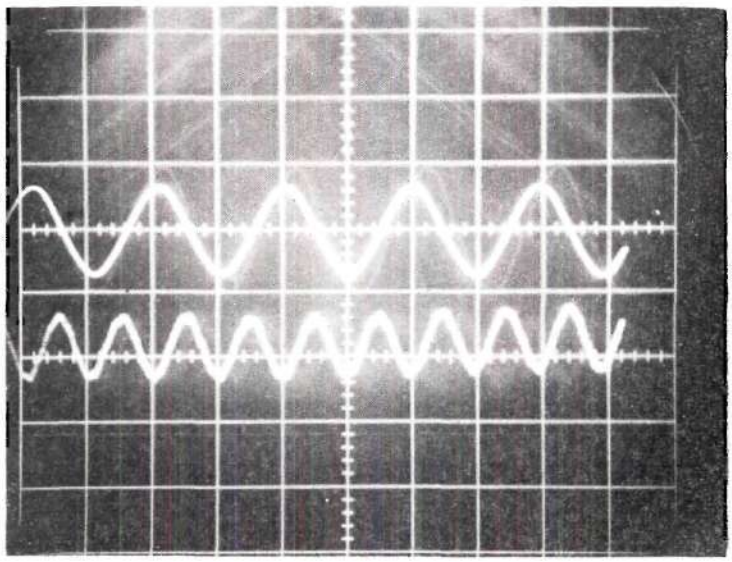

ℓ = 34.81 in. ω_2 = 10.4 cycles per second

d = 1.00 in.

h = 0.0625 in.

Figure 13. The Relationship between the Bending Strain (Top) and the Base Displacement (Bottom) for Second Mode Instability.

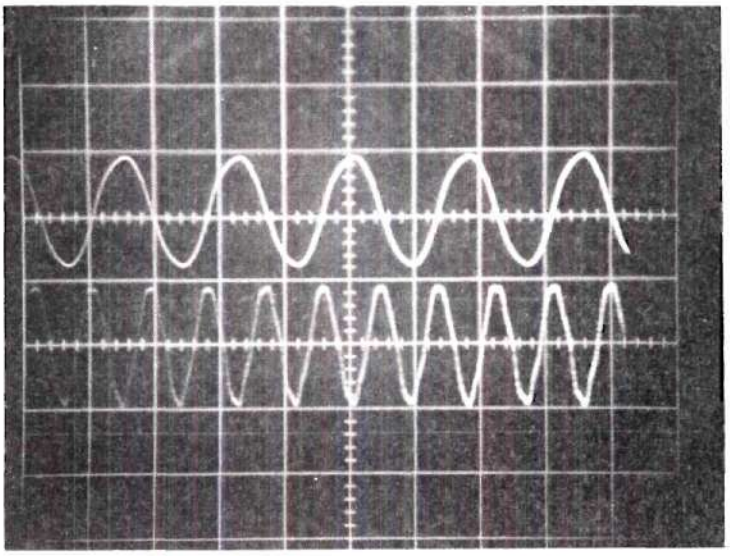

ℓ = 34.81 in. ω_3 = 29.5 cycles per second

d = 1.00 in.

h = 0.0625 in.

Figure 14. The Relationship between the Bending Strain (Top) and the Base Displacement (Bottom) for Third Mode Instability.

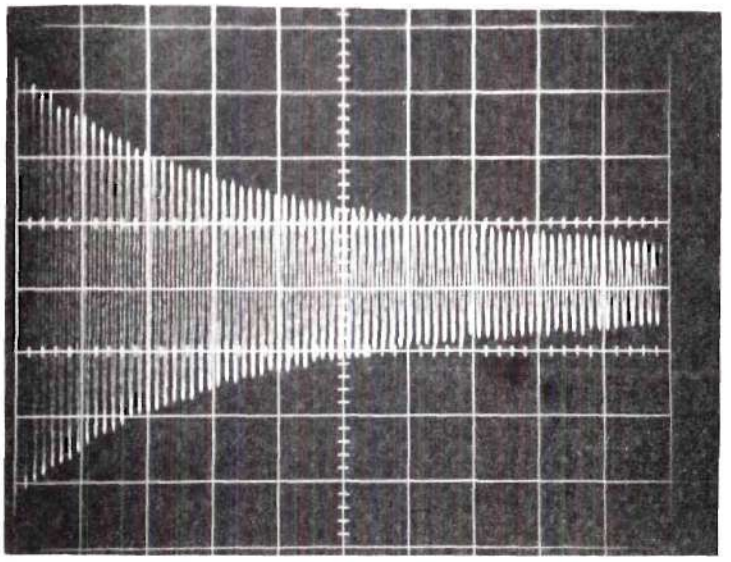

ℓ = 16.219 in. ω_1 = 3.77 cycles per second

d = 1.25 in. Δ_1 = 0.025

h = 0.03125 in.

Figure 15. Strain Trace of First Mode Damped Oscillations.

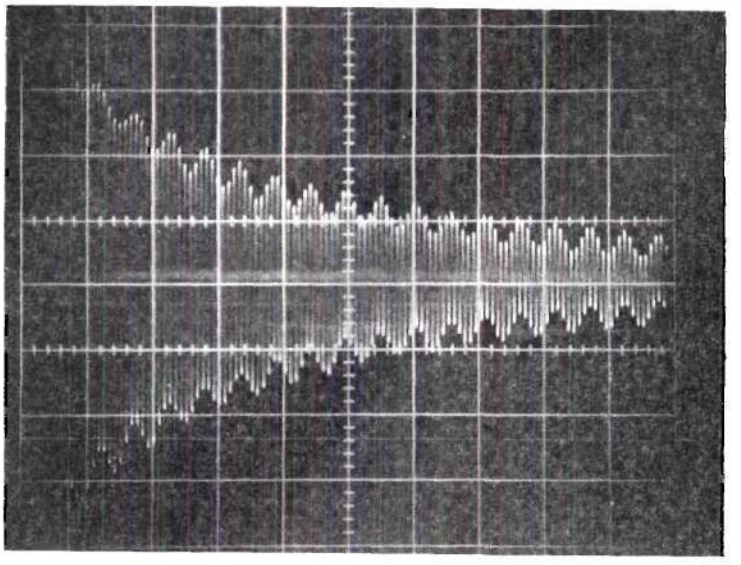

ℓ = 16.219 in. ω_2 = 24.0 cycles per second

d = 1.25 in. Δ_2 = 0.013

h = 0.03125 in.

Figure 16. Strain Trace of Second Mode Damped Oscillations.

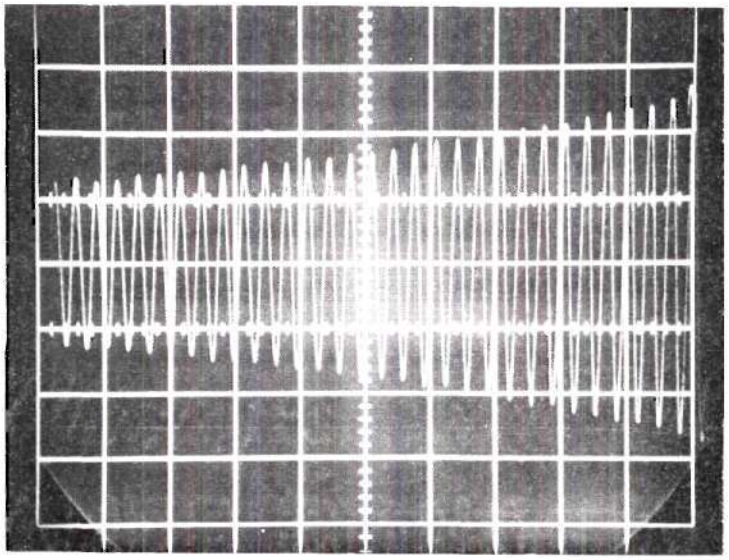

ℓ = 34.81 in. ω_1 = 1.56 cycles per second

d = 1.00 in. Δ_1 = 0.022

h = 0.0625 in.

Figure 17. Strain Trace of First Mode Damped Oscillations.

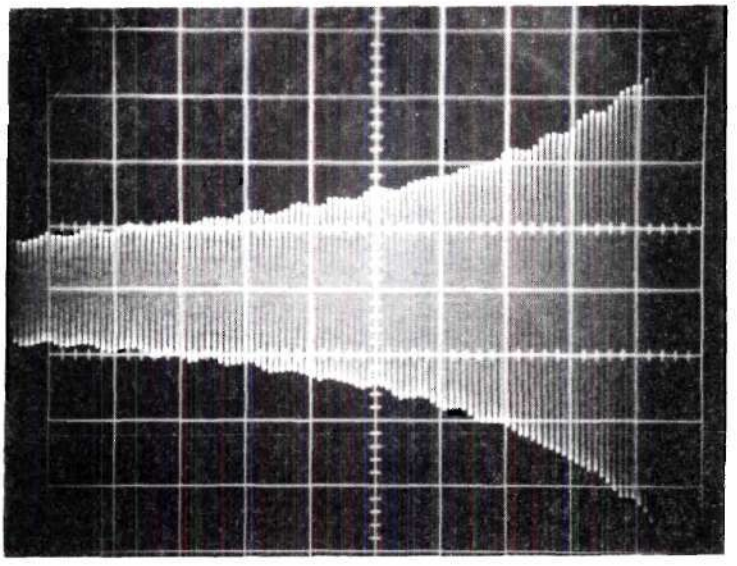

ℓ = 34.81 in. ω_2 = 10.4 cycles per second

d = 1.00 in. Δ_2 = 0.010

h = 0.0625 in.

Figure 18. Strain Trace of Second Mode Damped Oscillations.

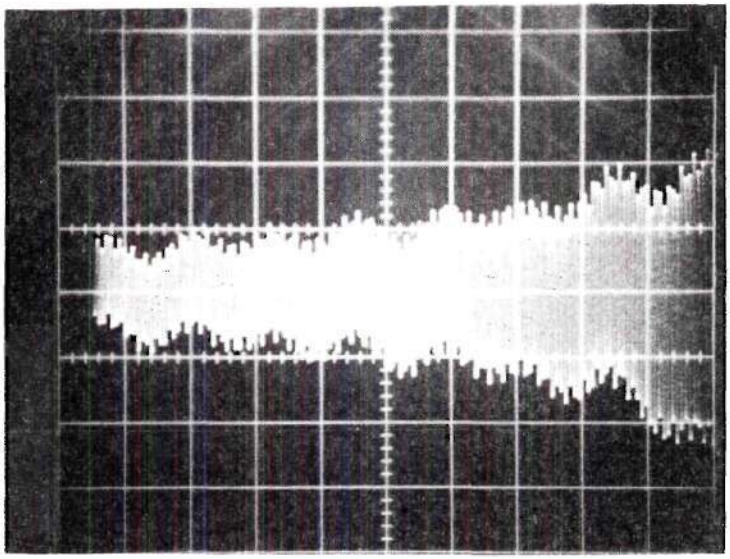

ℓ = 34.81 in. ω_3 = 29.5 cycles per second

d = 1.00 in. Δ_3 = 0.006

h = 0.0625 in.

Figure 19. Strain Trace of Third Mode Damped Oscillations.

Table 1. Experimental Second Mode Principal Instability Region for a 16 Inch Column

Length	ℓ = 16.219 in.	Mass Density	ρ = 485 lbm/ft^3
Width	d = 1.250 in.	Young's Modulus	E = 29.10^6 psi
Thickness	h = 0.03125 in.	ω_2	= 24.0 cps

Total Table Displacement (in.)	Table Frequency (rpm)		Maximum Table Acceleration (ft/sec^2)		$\frac{\Omega}{2\omega_2}$	
	Lower Instability Bound	Upper Instability Bound	Lower Instability Bound	Upper Instability Bound	Lower Instability Bound	Upper Instability Bound
.147	2830	3020	537.9	612.6	.983	1.049
.149	2820	3000	541.4	612.7	.979	1.042
.148	2810	3020	534.0	616.8	.976	1.049
.139	2815	3000	503.3	571.6	.977	1.042
.140	2810	3005	505.1	577.6	.976	1.043
.140	2820	3000	508.7	575.7	.979	1.042
.123	2840	3005	453.3	507.5	.986	1.043
.123	2820	3015	446.9	510.9	.979	1.047
.125	2845	3010	462.3	517.5	.988	1.045
.100	2860	3000	373.7	411.2	.993	1.042

(continued)

Table 1. Experimental Second Mode Principal Instability Region for a 16 Inch Column. (Continued)

Total Table Displacement (in.)	Table Frequency (rpm)		Maximum Table Acceleration (ft/sec^2)		$\frac{\Omega}{2\omega_2}$	
	Lower Instability Bound	Upper Instability Bound	Lower Instability Bound	Upper Instability Bound	Lower Instability Bound	Upper Instability Bound
.100	2860	2990	373.7	408.5	.993	1.038
.100	2860	2990	373.7	408.5	.993	1.038
.076	2860	2970	284.0	306.3	.993	1.031
.076	2870	2950	286.0	302.2	.996	1.024
.076	2880	2960	288.0	304.3	1.000	1.028
.048	2900	2960	184.5	192.2	1.007	1.028
.048	2880	2920	181.9	187.0	1.000	1.014
.050	2910	2940	193.5	197.5	1.010	1.021
.037	2930	2910	145.1	143.2	1.017	1.010
.037	2900	2920	142.2	144.1	1.007	1.014
.037	2900	2910	142.2	143.2	1.007	1.010
.022	2930	2930	86.3	86.3	1.017	1.017
.022	2930	2930	86.3	86.3	1.017	1.017

Table 2. Experimental Second Mode Principal Instability Region for a 35 Inch Column

Length	ℓ = 34.81 in.	Mass Density	ρ = 485 lbm/ft^3
Width	d = 1.00 in.	Young's Modulus	E = 29.10^6 psi
Thickness	h = 0.0625 in.	ω_2 = 10.4 cps	

Total Table Displacement (in.)	Table Frequency (rpm)		Maximum Table Acceleration (ft/sec^2)		$\frac{\Omega}{2\omega_2}$	
	Lower Instability Bound	Upper Instability Bound	Lower Instability Bound	Upper Instability Bound	Lower Instability Bound	Upper Instability Bound
.150	1280	1310	112.3	117.6	1.026	1.050
.150	1260	1280	108.8	112.3	1.010	1.026
.150	1260	1260	108.8	108.8	1.010	1.010
.150	1250	1250	107.1	107.1	1.002	1.002
.150	1240	1280	105.4	112.3	.994	1.026
.150	1250	1280	107.1	112.3	1.002	1.026
.150	1250	1260	107.1	108.8	1.002	1.010
.151	1250	1270	107.8	111.3	1.002	1.018
.127	1270	1320	93.6	101.1	1.018	1.058
.125	1260	1280	90.7	93.6	1.010	1.026

(Continued)

Table 2. Experimental Second Mode Principal Instability Region for a 35 Inch Column. (Continued)

Total Table Displacement (in.)	Table Frequency (rpm)		Maximum Table Acceleration (ft/sec^2)		$\frac{\Omega}{2\omega_2}$	
	Lower Instability Bound	Upper Instability Bound	Lower Instability Bound	Upper Instability Bound	Lower Instability Bound	Upper Instability Bound
.126	1250	1280	90.0	94.3	1.002	1.026
.100	1260	1270	72.5	73.7	1.010	1.018
.100	1230	1260	69.1	72.5	0.986	1.010
.100	1260	1270	72.5	73.7	1.010	1.018
.100	1240	1260	70.3	73.7	0.994	1.010
.100	1250	1260	71.4	73.7	1.002	1.010
.100	1250	1250	71.4	71.4	1.002	1.002
.100	1250	1260	71.4	73.7	1.002	1.010
.076	1260	1260	55.1	55.1	1.010	1.010
.077	1260	1265	55.1	56.3	1.010	1.014
.077	1280	1280	57.6	57.6	1.026	1.026
.074	1250	1260	52.8	53.7	1.002	1.010
.074	1220	1250	50.3	52.8	0.998	1.002
.074	1250	1260	52.8	53.7	1.002	1.010

(Continued)

Table 2. Experimental Second Mode Principal Instability Region for a 35 Inch Column. (Continued)

Total Table Displacement (in.)	Table Frequency (rpm)		Maximum Table Acceleration (ft/sec^2)		$\frac{\Omega}{2\omega_2}$	
	Lower Instability Bound	Upper Instability Bound	Lower Instability Bound	Upper Instability Bound	Lower Instability Bound	Upper Instability Bound
.068	1240	1250	47.8	48.6	0.994	1.002
.068	1260	1260	49.3	49.3	1.010	1.010
.050	1260	1260	36.3	36.3	1.010	1.010
.050	1270	1270	36.9	36.9	1.018	1.018
.051	1260	1260	37.0	37.0	1.010	1.010

Table 3. Experimental Third Mode Principal Instability Region for a 35 Inch Column

Length	ℓ = 34.81 in.	Mass Density	ρ = 485 lbm/ft^3
Width	d = 1.00 in.	Young's Modulus	E = 29.10^6 psi
Thickness	h = 0.0625 in.	ω_3	= 29.35 cps

Total Table-Displacement (in.)	Table Frequency (rpm)		Maximum Table Acceleration (ft/sec^2)		$\frac{\Omega}{2\omega_3}$	
	Lower Instability Bound	Upper Instability Bound	Lower Instability Bound	Upper Instability Bound	Lower Instability Bound	Upper Instability Bound
.151	3400	3760	797.6	975.4	0.965	1.068
.149	3370	3770	773.2	967.6	0.957	1.070
.150	3420	3790	801.7	984.5	0.971	1.076
.150	3260	3750	728.4	963.8	0.926	1.065
.150	3440	3780	811.1	979.3	0.977	1.073
.150	3360	3760	773.8	969.0	0.954	1.067
.150	3360	3750	773.8	963.8	0.954	1.065
.126	3430	3760	677.3	813.9	0.974	1.067
.126	3430	3740	677.3	805.3	0.974	1.062
.126	3420	3760	673.4	814.0	0.971	1.067

(Continued)

Table 3. Experimental Third Mode Principal Instability Region for a 35 Inch Column. (Continued)

Total Table Displacement (in.)	Table Frequency (rpm)		Maximum Table Acceleration (ft/sec^2)		$\frac{\Omega}{2\omega_3}$	
	Lower Instability Bound	Upper Instability Bound	Lower Instability Bound	Upper Instability Bound	Lower Instability Bound	Upper Instability Bound
.101	3460	3670	552.5	621.6	0.982	1.042
.101	3460	3670	552.5	621.6	0.982	1.042
.101	3450	3680	549.3	625.0	0.980	1.085
.100	3410	3650	531.3	608.7	0.968	1.036
.100	3400	3660	528.2	612.1	0.965	1.039
.100	3390	3640	525.1	605.4	0.963	1.034
.077	3500	3670	431.0	473.9	0.994	1.042
.076	3500	3660	425.4	365.2	0.994	1.039
.076	3490	3670	423.0	467.7	0.991	1.042
.074	3450	3600	402.5	438.2	0.980	1.022
.074	3450	3600	402.5	438.2	0.980	1.022
.074	3440	3600	400.1	438.2	0.977	1.022
.068	3480	3630	376.3	409.4	0.988	1.031
.068	3540	3620	389.4	389.4	1.005	1.028

(Continued)

Table 3. Experimental Third Mode Principal Instability Region for a 35 Inch Column. (Continued)

Total Table Displacement (in.)	Table Frequency (rpm)		Maximum Table Acceleration (ft/sec^2)		$\frac{\Omega}{2\omega_3}$	
	Lower Instability Bound	Upper Instability Bound	Lower Instability Bound	Upper Instability Bound	Lower Instability Bound	Upper Instability Bound
.068	3460	3590	372.0	400.5	0.982	1.019
.050	3460	3520	273.5	283.1	0.982	0.999
.050	3490	3610	278.3	297.7	0.991	1.025
.050	3520	3620	283.1	299.4	0.999	1.028
.050	3520	3620	283.1	299.4	0.999	1.028
.051	3650	3640	310.5	308.8	1.036	1.034
.051	3600	3640	302.0	308.8	1.022	1.034
.037	3520	3590	209.5	217.9	0.999	1.019
.037	3500	3590	207.1	217.9	0.994	1.019
.037	3500	3560	207.1	214.3	0.994	1.011
.036	3540	3560	206.1	208.5	1.005	1.011
.035	3500	3520	195.9	198.2	0.994	0.999
.034	3500	3540	190.3	194.7	0.994	1.005

APPENDIX II

COMPUTER METHODS AND RESULTS

Much of the success of the analytical part of this thesis depends upon the use of a digital computer to carry out the routine repetitive operations. The computer program can be broken into the two following main divisions with each division having subsequent parts:

1. Derive the governing Mathieu's equation.
   a. Use equations (30-33) from the boundary conditions and the "method of false positions" [15] to find the first n natural frequencies of free vibration ω_n and the constants A, B, C, and D in the free vibration mode shape $\psi_n(x)$.
   b. Use the results of part 1a to evaluate the integrals from the Galerkin analysis in Chapter III. This gives the constants α, β, and γ, the coefficients of the Mathieu's equation (38).
2. Calculate the regions of instability.
   a. Use the power series expansion for the instability regions as given in McLachlan [7] to plot undamped stability charts. The first section of Chapter IV showed that if a value of base amplitude A_p is given, a value of the forcing frequency Ω bounding the instability region can be found. For the analysis presented in this paper, the

maximum base acceleration $A_p\Omega^2$ is plotted as the abscissa, and $\frac{\Omega}{2\omega_n}$ is plotted as the ordinate for the instability regions.

b. Calculate the damping decrement Δ_n in each mode from strain trace of damped oscillations. See Figures 15-19. Use this decrement in equations (45) to determine the instability boundaries for damped vibrations. Since the variable μ contains the maximum base acceleration $A_p\Omega^2$, stability charts of $\frac{\Omega}{2\omega_n}$ versus $A_p\Omega^2$ can be plotted as in part 2a.

```
BEGIN
$$ A A069                                                                    00000000
                                                                             99999999

FILE IN  MECK (2,10) ; %
FILE OUT PRINT 4(3,15) ; %
INTEGER       N,NN,NNN,JJ,T,TT,NUMBER ; %
REAL      E,ESI,L,LI,H,HI,W,WI,RHOL,RHO,ML,M,JLB,J,I,AREA,
          TMASSI,TMASS,LMASSI,LMASS,ECCI,ECC,DELTA,
          SINE,COSINE,SINH,COSH,OMEGA,AMPLITUDE,PART,KK1,KK2,PI,PI2,
          A,B,C,D,AA,BB,CC,DD,EE,FF,GG,HH,TEMP,
          N1S,N2S,N3S,OMEGAMAX,XGA,
          LA1,LA2,LA3,LA4,LA5,LA6,LA7,LA8,A1,KK,K,KING ; %
REAL ARRAY    X,XX,DET,DUM[0:300],
              DEK,STRAIN,ACCMAX[0:5], %
              S,COEFF1,COEFF2,KING1,KING2[0:2] ; %
FORMAT        FMT1(//  ,X45,"NATURAL",X22,"NATURAL",/,
                       X44,"FREQUENCY",X20,"FREQUENCY",/,
                       X45,"NUMBER",X17,"(CYCLES PER SECOND)") ,
              FMT2(///  ,X55,"MODE SHAPE"),
              FMT3(//,X48,"X",X24,"MODE SHAPE",X11,/,
                     X46,"(IN.)",X17,"RELATIVE DEFLECTION",X9,/ ) ,
              FMT4(///,X61,"MATHIEU S EQUATION") ,
              FMT5(/  ,X47,"T (T)",X12,"      COS(    )XT(T)",X12,
                       "T(T)" ),
              FMT6(//////   ,X60,"OUTPUT DATA", ) ,
              FMT7(/////////,X73,"INPUT DATA",///),
              FMT8(    X70,"COLUMN VARIABLES"),
              FMT9(  /,X44,"LENGTH",X7 ,"WIDTH",X7 ,"THICKNESS",X7 ,
                       "DENSITY",X7 ,"YOUNG S MODULUS"),
              FMT10( X45,"(IN)",X8 ,"(IN)",X11,"(IN)",X8 ,
                       "(LBM/FT*3)"  ,X8 ,"(LB/IN*2)"),
              FMT11(////,X68,"END MASS VARIABLES",/ ) ,
              FMT12(   X49,"END MASS",X7 ,"ECCENTRICITY",X7 ,
                       "MOMENT OF INERTIA"),
              FMT13(   X51,"(LB)",X13,"(IN)",X14,"(LBM FT*2)" ) ,
              FMT14(   ,X62,"PRINCIPAL INSTABILITY REGION" ),
              FMT15(   ,X64,"SECOND INSTABILITY REGION" ) ,
```

```
                FMT16(    ,X64,"THIRD INSTABILITY REGION" ) ,
                FMT17(// ,X72,"UNDAMPED" ),
                FMT18(// ,X72," DAMPED " ) , %
                FMT19(/ ,X49,"BASE",X12,"LOWER",X12,"BASE",X12,"UPPER",/,
                     X46,"ACCELERATION",X4,"INSTABILITY",X6,"ACCELERATION"
                     ,X4,"INSTABILITY",/,X46,"(FT./SEC*2)",X8,"BOUND",X9,
                     "(FT./SEC*2)",X8,"BOUND",/ ) ,
                FMT20(/ ,    X49,"BASE",X19,"LOWER",X19,"UPPER",/,X46,
                     "ACCELERATION",X11,"INSTABILITY",X13,"INSTABILITY",
                     /,X46,"(FT./SEC*2)",X15,"BOUND",X19,"BOUND", / ) ,
                FMT21(///,X60,"EXPERIMENTAL DATA" ) ,
                       FMT22(/ ,X60,"DAMPING DECREMENT" ) ; %
FORMAT OUT      FMT01(/,X47,I1,X25,F6.2) ,
                FMT03( X46,F5.2,X24,F6.2,X15,F6.2 ),
                FMT05(/,X47,F4.2,X16,E11.4,X14,E11.4),
                FMT06( X44,F6.4,X17,3(X6 ,E11.4)),
                FMT07(X46,2(E11.4  ,X7 ,F7.5,X8 ) ) ,
                FMT07D(X46,E11.4, X14,F7.5,X17,F7.5) ,
                FMTOEXP(/  ,X66,F5.3, X18,F4.2,X18,E11.4,///) ,
                FMTI9( X44,F6.3,X7 ,F5.3,X9 ,F6.4,X9 ,F5.1,X11,E8.1),
                FMTI12( X51,F4.2,X13,F4.2,X16,F6.4) ; %
%
LIST            LSTIN(ESI,LI,WI,HI,RHOL,LMASSI,TMASSI,ML,ECCI,
                      X[1],DELTA,TT,NN,NUMBER,AMPLITUDE,XGA,
                      FOR T ← 1 STEP 1 UNTIL TT DO ACCMAX[T] ,
                      FOR T ← 1 STEP 1 UNTIL TT DO DEK[T] ,
                      FOR T ← 1 STEP 1 UNTIL TT DO STRAIN[T] ) ; %
%
READ(MECK,/,LSTIN) ;
WRITE(PRINT[NO]) ; %
%
BEGIN %
REAL ARRAY      NAT,C01,C02,C03,MAD,MBD,MCD,MDD[0:TT],
                DEFL,DEFA[0:TT,0:NN] ,
                AC1,AC2,AC3[0:NUMBER],
          OSA1C,OSA2C,OSA3C,OSB1S,OSB2S,OSB3S,
                           ACB1S,ACB2S,ACB3S,ACA1C,ACA2C,ACA3C,
```

```
          DA1C,DA2C,DA3C,DB1S,DB2S,DB3S[0:TT,0:NUMBER] ; %
LABEL     RETURN,COMPLETE, CHECK ; %
%
REAL PROCEDURE      MAXVALUE(A,T,NN) ; %
VALUE               NN,T ; %
INTEGER             NN, T ; %
REAL ARRAY          A[0,0] ; %
BEGIN %
INTEGER             N    ; %
REAL                TEMP ; %
LABEL               REPEAT,ALLTHROUGH ; %
N ← 0 ; %
TEMP ← ABS(A[T,1]) ; %
REPEAT:  N ← N + 1 ; %
          IF N = NN %
          THEN GO TO ALLTHROUGH ; %
          IF TEMP < ABS(A[T,N+1]) %
          THEN    BEGIN
                  TEMP ← ABS(A[T,N+1]) ; %
                  GO TO REPEAT ; %
                  END %
        ELSE      GO TO REPEAT ; %
ALLTHROUGH:
MAXVALUE ← TEMP ; %
END ; %
PROCEDURE      STABCHART(OSB1S,OSB2S,OSB3S,OSA1C,OSA2C,OSA3C,
                         ACB1S,ACB2S,ACB3S,ACA1C,ACA2C,ACA3C,
                         NNN,T,AMPLITUDE,NUMBER) ; %
VALUE               T,NUMBER ; %
INTEGER             T,NUMBER,NNN ; %
REAL                AMPLITUDE ; %
REAL ARRAY          OSB1S,OSB2S,OSB3S,OSA1C,OSA2C,OSA3C,
                    ACB1S,ACB2S,ACB3S,ACA1C,ACA2C,ACA3C[0,0] ; %
BEGIN %
REAL                TEMP,Q ; %
INTEGER             N ; %
REAL ARRAY          B1S,B2S,B3S,A1C,A2C,A3C[0:T,0:NUMBER] ;
```

```
LABEL          HELP ; %
TEMP ← 4 × NAT[T]*2 ; %
FOR N ← 0 STEP 1 UNTIL NUMBER DO
BEGIN
Q ← - 2 × CO3[T]/CO1[T] × AMPLITUDE × N / NUMBER ; %
B1S[T,N]←1 - Q - Q*2/8 + Q*3/64 - Q*4/1536 - 11×Q*5/36864 +
          49×Q*6/589824 -55×Q*7/9437184 -265×Q*8/113246208 ;
A1C[T,N]←1 + Q - Q*2/8 - Q*3/64 - Q*4/1536 + 11×Q*5/36864 +
          49×Q*6/589824 +55×Q*7/9437184 -265×Q*8/113246208 ;
B2S[T,N]←4 - Q*2/12 + 5×Q*4/13824 - 289×Q*6/79626240 + 21391×Q*8/
          458647142400 ;
A2C[T,N]←4 + 5×Q*2/12 - 763×Q*4/13824 + 10.02401×Q*6/796.26240 -
          1.669068401×Q*8/458.647142400 ;
B3S[T,N]←9 + Q*2/16 - Q*3/64 + 13×Q*4/20480 + 5×Q*5/16384 -
          1.961×Q*6/23592.960 +6.09×Q*7/1048576.00 ;
A3C[T,N]←9 + Q*2/16 + Q*3/64 + 13×Q*4/20480 - 5×Q*5/16384 -
          1.961×Q*6/23592.960 -6.09×Q*7/1048576.00 ;
IF TEMP/B1S[T,N] < 0 THEN GO TO HELP ; %
IF TEMP/B2S[T,N] < 0 THEN GO TO HELP ; %
IF TEMP/B3S[T,N] < 0 THEN GO TO HELP ; %
IF TEMP/A1C[T,N] < 0 THEN GO TO HELP ; %
IF TEMP/A2C[T,N] < 0 THEN GO TO HELP ; %
IF TEMP/A3C[T,N] < 0 THEN GO TO HELP ; %
NNN ← N ; %
OSB1S[T,N] ← B1S[T,N] ; %
OSA1C[T,N] ← A1C[T,N] ; %
OSB2S[T,N] ← B2S[T,N] ; %
OSA2C[T,N] ← A2C[T,N] ; %
OSB3S[T,N] ← B3S[T,N] ; %
OSA3C[T,N] ← A3C[T,N] ; %
ACB1S[T,N]     ←      (TEMP / B1S[T,N]) × AMPLITUDE × N / NUMBER ; %
ACA1C[T,N]     ←      (TEMP / A1C[T,N]) × AMPLITUDE × N / NUMBER ; %
ACB2S[T,N]     ←      (TEMP / B2S[T,N]) × AMPLITUDE × N / NUMBER ; %
ACA2C[T,N]     ←      (TEMP / A2C[T,N]) × AMPLITUDE × N / NUMBER ; %
ACB3S[T,N]     ←      (TEMP / B3S[T,N]) × AMPLITUDE × N / NUMBER ; %
ACA3C[T,N]     ←      (TEMP / A3C[T,N]) × AMPLITUDE × N / NUMBER ; %
END ; %
```

```
HELP: %
END ; %
PROCEDURE      DAMPING(DB1S,DB2S,DB3S,N1S,N2S,N3S,AC1,AC2,AC3,
                       ACCMAX,DEK,NUMBER,T ) ; %
VALUE          NUMBER,T  ; %
INTEGER        N1S,N2S,N3S,T,NUMBER ; %
REAL ARRAY     DB1S,DB2S,DB3S[0,0],AC1,AC2,AC3,DEK,ACCMAX[0] ; %
BEGIN %
REAL      DELACC,DELMU,TEMP1,TEMP2,TEST1,TEST2,DEC,
          MU1,MU2,MU3,MU1S,MU2S,MU3S ; %
LABEL          HOP1,HOP2,HOP3 ; %
INTEGER  N ; %
DEC ← DEK[T] ; %
DELACC ← ACCMAX[T]/NUMBER ; %
DELMU ← - DELACC × (CO3[T]/CO1[T]) /(2×NAT[T]*2) ; %
DELMU ← ABS(DELMU) ; %
MU1S ←         (DEC/PI)       ; %
MU2S ←         (DEC/PI)*.50   ; %
MU3S ←         (DEC/PI)*.3333; %
N ← 0 ; %
FOR MU1 ← MU1S STEP DELMU UNTIL 1000 DO %
BEGIN %
TEST1 ←                          SQRT((MU1     )*2 - (DEC/PI)*2) ; %
IF TEST1 > 1 THEN GO TO HOP1 ; %
IF N+1 > NUMBER THEN GO TO HOP1 ; %
N1S ← N ← N + 1 ; %
AC1[N] ←ABS(-2×NAT[T]*2 × CO1[T]/CO3[T] × MU1S)+ DELACC× (N -1) ;
          DB1S[T,N] ← SQRT(1 + SQRT((MU1     )*2 - (DEC/PI)*2)) ; %
          DA1C[T,N] ← SQRT(1 - SQRT((MU1     )*2 - (DEC/PI)*2)) ; %
END ; %
HOP1: %
N ← 0 ; %
FOR  MU2 ← MU2S STEP DELMU UNTIL 1000 DO %
BEGIN  %
TEST2 ←                          +(MU2     )*2 + SQRT((MU2     )*4
          - (DEC/PI)*2 × (1 -(MU2     )*2) ) ; %
IF TEST2 > 1 THEN GO TO HOP2 ; %
```

```
IF N+1 > NUMBER THEN GO TO HOP2 ; %
N2S ← N ← N + 1 ; %
AC2[N] ←ABS(-2×NAT[T]*2 × CO1[T]/CO3[T] × MU2S)+ DELACC× (N -1) ;
        DB2S[T,N] ←  SQRT(1 -(MU2    )*2 + SQRT((MU2    )*4
        - (DEC/PI)*2 × (1 -(MU2    )*2) ) )/2 ; %
        DA2C[T,N] ←  SQRT(1 -(MU2    )*2 - SQRT((MU2    )*4
        - (DEC/PI)*2 × (1 -(MU2    )*2) ) )/2 ; %
END ; %
HOP2: %
N ← 0 ; %
FOR  MU3 ← MU3S STEP DELMU UNTIL 1000 DO %
BEGIN
TEMP1←(8×(MU3    )*2 /9  +  SQRT( (MU3    )*6  - (DEC/PI)*2 ×
      ( 64/81 - 2 × (MU3    )*2/3 )))/( 64/81 - (MU3    )*2) ;
TEMP2←(8×(MU3    )*2 /9  -  SQRT( (MU3    )*6  - (DEC/PI)*2 ×
      ( 64/81 - 2 × (MU3    )*2/3 )))/( 64/81 - (MU3    )*2) ;
IF TEMP1 > 1 THEN GO TO HOP3 ; %
IF TEMP2 > 1 THEN GO TO HOP3 ; %
IF N+1 > NUMBER THEN GO TO HOP3 ; %
N3S ← N ← N + 1 ; %
AC3[N] ←ABS(-2×NAT[T]*2 × CO1[T]/CO3[T] × MU3S)+ DELACC× (N -1) ;
        DB3S[T,N] ← SQRT(1 - TEMP2)/3 ;
        DA3C[T,N] ← SQRT(1 - TEMP1)/3 ;
END ; %
HOP3: %
END ; %
PROCEDURE      DEFLECTION(MAD,MBD,MCD,MDD,NAT,DEFA,
                          T,H,XGA,STRAIN) ; %
VALUE          T,H,XGA  ; %
INTEGER        T ; %
REAL           H,XGA ; %
REAL ARRAY     MAD,MBD,MCD,MDD,NAT,STRAIN[0],DEFA[0,0] ; %
BEGIN %
REAL           K,XGF ; %
INTEGER        JJ ; %
REAL ARRAY     YDP,CONST[0:TT] ; %
XGF ← XGA/12 ; %
```

```
K ← SQRT(NAT[T]/A1) ; %
YDP[T] ←  K*2 × (-MAD[T] × COS(XGF×K)
                 -MBD[T] × SIN(XGF×K)
                 +MCD[T] × HYPERBOLIC("COS",XGF×K)
                 +MDD[T] × HYPERBOLIC("SIN",XGF×K)); %
CONST[T] ←  STRAIN[T]/(H×YDP[T]/2) ; %
FOR JJ ← 0 STEP 1 UNTIL NN DO %
DEFA[T,JJ] ← (MAD[T] × COS(K×PART×JJ) +
              MBD[T] × SIN(K×PART×JJ) +
              MCD[T] × HYPERBOLIC("COS",K×PART×JJ) +
              MDD[T] × HYPERBOLIC("SIN",K×PART×JJ))×CONST[T] ; %
END ; %
LIST          INLST9( LI,WI,HI,RHOL,ESI) ; %
LIST          INLST12(ML,ECCI,JLB) ; %
LIST          LST1(T , NAT[T]/(2×3.14159)) ;
LIST          LST3( PART × JJ × 12 , DEFL[T,JJ] × 10 ) ; %
LIST          LST5(1  ,C03[T]/C01[T],NAT[T]*2 ) ; %
LIST          LST7( ACB1S[T,JJ],SQRT(1/DSB1S[T,JJ]) ,
                    ACA1C[T,JJ],SQRT(1/DSA1C[T,JJ] )) ; %
LIST          LST8( ACA2C[T,JJ],SQRT(1/DSA2C[T,JJ] ),
                    ACB2S[T,JJ],SQRT(1/DSB2S[T,JJ])) ; %
LIST          LST9( ACB3S[T,JJ],SQRT(1/DSB3S[T,JJ]) ,
                    ACA3C[T,JJ],SQRT(1/DSA3C[T,JJ] )) ; %
LIST          LSD7( AC1[JJ],DA1C[T,JJ], DB1S[T,JJ]) ; %
LIST          LSD8( AC2[JJ],DA2C[T,JJ], DB2S[T,JJ]) ; %
LIST          LSD9( AC3[JJ],DA3C[T,JJ], DB3S[T,JJ]) ; %
LIST          LSTEXP(DEK[T]) ; %
%
PI ← 3.14159 ; %
PI2 ← 2 × 3.14159 ; %
E ← ESI × 144 ; %
L ← LI/12 ; %
W ← WI/12 ; %
H ← HI/12 ; %
AMPLITUDE ← AMPLITUDE/12 ; %
RHO ← RHOL/32.2 ; %
M ← ML/32.2 ; %
```

```
ECC ← ECCI/12 ; %
LMASS ← LMASSI/12 ; %
TMASS ← TMASSI/12 ; %
JLB ← ML × ( LMASS*2 + TMASS*2 )/12 ; %
J ← JLB/32.2 ; %
%
AREA ← W × H ; %
I ←  W × H*3/12 ; %
A1← SQRT(E×I/(AREA×RHO)) ; %
PART ← L/NN ; %
%
% THIS PART OF THE PROGRAM COMPUTES THE NATURAL FREQUENCIES OF A
% CANTILEVER BEAM WITH A MASS ATTACHED AT THE END
N ← 1 ; %
T ← 1 ; %
RETURN: %
OMEGA ← X[N] ; %
KK← SQRT( OMEGA/A1); %
AA ← E × I ×KK*3 ; %
BB ← E × I ×KK*2 ; %
CC ←KK × J × OMEGA*2 ; %
DD ←KK × L ; %
EE ← M × OMEGA*2 ; %
FF ←  EE × KK × ECC ; %
GG ←  EE × ECC ; %
HH ←  GG × KK × ECC ; %
SINE ←   SIN(DD) ; %
COSINE ← COS(DD) ; %
SINH ←   HYPERBOLIC("SIN",DD) ; %
COSH ←   HYPERBOLIC("COS",DD) ; %
%
LA1 ← ( AA -  FF) × SINE +  EE × COSINE ; %
LA2 ← (-AA +  FF) × COSINE +  EE × SINE ; %
LA3 ← ( AA +  FF) × SINH   +  EE × COSH ; %
LA4 ← ( AA +  FF) × COSH   +  EE × SINH ; %
LA5 ← (+BB +  GG) × COSINE +  (-CC - HH) × SINE ; %
LA6 ← (+BB +  GG) × SINE   +  ( CC + HH) × COSINE ; %
```

```
LA7 ← (-BB +  GG) × COSH  +   ( CC + HH) × SINH ; %
LA8 ← (-BB +  GG) × SINH  +   ( CC + HH) × COSH ; %
DET[N] ←  LA3 × LA8 - LA7 × LA4  +
          LA2 × LA7 - LA3 × LA6  +
          LA5 × LA4 - LA1 × LA8 +
          LA1 × LA6 - LA5 × LA2 ;%
%
IF N=1 %
THEN      BEGIN %
          N ← 2 ; %
          X[N] ← X[N-1] + DELTA ; %
          GO TO RETURN ; %
          END ; %
%
IF SIGN(DET[N]) = SIGN(DET[N-1]) %
THEN      BEGIN N ← N+1 ; X[N] ← X[N-1] + DELTA ; GO TO RETURN ; END
ELSE      BEGIN
          CHECK:
          IF (X[N]-X[N-1])≤.05
          THEN GO TO COMPLETE
          ELSE BEGIN
          XX[N] ← (X[N-1] × DET[N] - X[N] × DET[N-1] )/
                   ( DET[N] - DET[N-1]) ;
OMEGA ←XX[N] ; %
KK← SQRT( OMEGA/A1); %
AA ← E × I ×KK*3 ; %
BB ← E × I ×KK*2 ; %
CC ←KK × J × OMEGA*2 ; %
DD ←KK × L ; %
EE ← M × OMEGA*2 ; %
FF ←  EE × KK × ECC ; %
GG ←  EE × ECC ; %
HH ←  GG × KK × ECC ; %
SINE ←   SIN(DD) ; %
COSINE ← COS(DD) ; %
SINH ←   HYPERBOLIC("SIN",DD) ; %
COSH ←   HYPERBOLIC("COS",DD) ; %
```

```
LA1 ← ( AA -  FF) × SINE +  EE × COSINE ; %
LA2 ← (-AA +  FF) × COSINE +  EE × SINE ; %
LA3 ← ( AA +  FF) × SINH   +  EE × COSH ; %
LA4 ← ( AA +  FF) × COSH   +  EE × SINH ; %
LA5 ← (+BB +  GG) × COSINE +  (-CC - HH) × SINE ; %
LA6 ← (+BB +  GG) × SINE   +  ( CC + HH) × COSINE ; %
LA7 ← (-BB +  GG) × COSH   +  ( CC + HH) × SINH ; %
LA8 ← (-BB +  GG) × SINH   +  ( CC + HH) × COSH ; %
%
DUM[N] ←  LA3 × LA8 - LA7 × LA4  +
          LA2 × LA7 - LA3 × LA6  +
          LA5 × LA4 - LA1 × LA8  +
          LA1 × LA6 - LA5 × LA2 ;%
%
%
IF SIGN(DUM[N]) = SIGN(DET[N])
THEN      BEGIN %
          X[N] ← XX[N] ; %
          DET[N] ← DUM[N] ; %
          END %
ELSE      BEGIN %
          X[N-1] ← XX[N] ; %
          DET[N-1] ← DUM[N] ; %
          END;%
%
GO TO CHECK ; %
          END ; %
          END ;
COMPLETE:
     NAT[T] ← X[N] ; %
     MAD[T] ← 1 ; %
     MBD[T] ← (LA1 - LA3)/(LA4 - LA2) ; %
     MCD[T] ← -1 ; %
     MDD[T] ← - MBD[T] ; %
%
          IF T< TT THEN BEGIN %
           N ← 1 ; %
```

```
          X[1] ← NAT[ T ] + DELTA ; %
          T ← T + 1 ; %
          GO TO RETURN ; END ; %
%
% END OF NATURAL FREQUENCY CALCULATIONS
%
%
% THIS PART OF THE PROGRAM COMPUTES THE COEFFICIENTS IN MATHIEU S
% EQUATION
FOR T ← 1 STEP 1 UNTIL TT DO BEGIN %
    K ←  SQRT(NAT[T]/A1) ; %
A   ←  MAD[T] ; %
B   ←  MBD[T] ; %
C   ←  MCD[T] ; %
D   ←  MDD[T] ; %
S[2] ← L ; S[1] ← 0 ; %
FOR N ← 1,2 DO BEGIN  %
COEFF1[N]     ← (A*2 + B*2) × S[N]/2  + (A*2 - B*2) × SIN(2×K×S[N])/
                (4×K) +  A×B×(SIN(K×S[N]))*2/K +2 × A × D × (
                HYPERBOLIC("SIN",K×S[N]) × SIN(K×S[N])/K) +
              (A×C - B×D) × HYPERBOLIC("SIN",K×S[N]) × COS(K × S[N])/K
            + (A×C + B×D) × HYPERBOLIC("COS",K×S[N]) × SIN(K × S[N])/K
            + (C*2 + D*2) × HYPERBOLIC("SIN",2×K×S[N])/(4×K)
            + (C*2 - D*2) × S[N]/2 +  C × D × (HYPERBOLIC("SIN",K×S[N]
              ))*2/K  ; %
KING1[N]←K*2 × ( -(A*2 - B*2) × SIN(2×K×S[N]) /(4×K) + B*2 × S[N]
      +  A × B × COS(2×K×S[N])/(2×K) + ( C*2 + D*2) ×
         HYPERBOLIC("SIN",2×K×S[N])/(4×K) + C × D  ×
         HYPERBOLIC("COS",2×K×S[N])/(2×K)   +
     1/K × ( - A×C ×( HYPERBOLIC("COS",K×S[N]) ×  SIN(K×S[N])
                     -HYPERBOLIC("SIN",K×S[N]) ×  COS(K×S[N]) )
             - A×D ×( HYPERBOLIC("SIN",K×S[N]) ×  SIN(K×S[N])
                     -HYPERBOLIC("COS",K×S[N]) ×  COS(K×S[N]) )
             + B×C ×( HYPERBOLIC("COS",K×S[N]) ×  COS(K×S[N])
                     +HYPERBOLIC("SIN",K×S[N]) ×  SIN(K×S[N]) )
             + B×D ×( HYPERBOLIC("SIN",K×S[N]) ×  COS(K×S[N])
                     +HYPERBOLIC("COS",K×S[N]) ×  SIN(K×S[N]) ) ) ) ; %
```

```
KING2[N] ← K*2 × (  -(A*2 - B*2)/2 × ( COS(2×K×S[N])/(2×K)*2  + S[N] ×
                    SIN(2×K×S[N])/(2×K) ) + B*2 × S[N]*2 /2
                    - A × B × ( SIN(2×K×S[N])/(2×K)*2 - S[N] ×
                    COS(2×K×S[N])/(2×K) ) +  ( C*2 + D*2)/2 ×
                    ( S[N] × HYPERBOLIC("SIN",2×K×S[N])/(2×K)
                   - HYPERBOLIC("COS",2×K×S[N])/(2×K)*2 ) + C × D ×
                    ( S[N] × HYPERBOLIC("COS",2×K×S[N])/(2×K)
                   - HYPERBOLIC("SIN",2×K×S[N])/(2×K)*2 )
+  (- A×(C + D) × ( S[N] × EXP(K×S[N]) × ( SIN(K×S[N]) - COS(K×S[N]) )
                   + EXP(K×S[N]) × COS(K×S[N])/K )
    - A×(D - C) × ( S[N] × EXP(-K×S[N]) ×(-SIN(K×S[N]) - COS(K×S[N]) )
                   - EXP(-K×S[N])× COS(K×S[N])/K )
    + B×(C + D) × ( S[N] × EXP(K×S[N]) × ( COS(K×S[N]) + SIN(K×S[N]) )
                   - EXP(K×S[N]) × SIN(K×S[N])/K )
    + B×(D - C) × ( S[N] × EXP(-K×S[N]) ×(-COS(K×S[N]) + SIN(K×S[N]) )
                   + EXP(-K×S[N])× SIN(K×S[N])/K ) ) / (2 × K) ) ; %
              END ; %
%
% CO1[T] = THE COEFFICIENT OF THE SECOND DERIVATIVE OF THE
% "FUNCTION OF TIME" IN MATHIEU S EQUATION FOR THE "T"TH MODE SHAPE
CO1[T]←(COEFF1[2] - COEFF1[1])× RHO × AREA ; %
%
%CO2[T] = THE COEFFICIENT OF  THE "FUNCTION OF TIME" IN
% MATHIEU S EQUATION FOR THE "T"TH MODE SHAPE
CO2[T]←(COEFF1[2] - COEFF1[1])× E × I × K*4 ; %
%
%CO3[T] = THE COEFFICIENT OF COS(OMEGAF × T) TIMES THE
% "FUNCTION OF TIME" IN MATHIEU S EQUATION FOR THE "T"TH MODE SHAPE
KING ← (A × COS( K × L) + B × SIN( K × L) +
        C × HYPERBOLIC("COS",K × L) + D × HYPERBOLIC("SIN",K × L) ) × K
   ×  (-A × SIN( K × L) + B × COS( K × L) +
        C × HYPERBOLIC("SIN",K × L) + D × HYPERBOLIC("COS",K × L)) ;
KK1 ← M + L × RHO × AREA ; %
KK2 ← - RHO × AREA ; %
CO3[T]←-(KING × ( KK1 + L × KK2) - KK1 × (KING1[2] - KING1[1]) -
                                   KK2 × (KING2[2] - KING2[1]))) ; %
%
```

```
%
K ← SQRT(NATIT]/A1) ; %
%
FOR JJ ← 0 STEP 1 UNTIL NN DO %
BEGIN %
DEFL[T,JJ] ←  MAD[T] × COS(K×PART×JJ) +
              MBD[T] × SIN(K×PART×JJ) +
              MCD[T] × HYPERBOLIC("COS",K×PART×JJ) +
              MDD[T] × HYPERBOLIC("SIN",K×PART×JJ) ; %
END ;%
%
TEMP ← MAXVALUE(DEFL,T,NN) ; %
FOR JJ ← 0 STEP 1 UNTIL NN DO
DEFL[T,JJ]← DEFL[T,JJ]/TEMP ; %
END ;%
%
WRITE(PRINT,FMT7) ; %
WRITE(PRINT,FMT8) ; %
WRITE(PRINT,FMT9) ; %
WRITE(PRINT,FMT10) ; %
WRITE(PRINT,FMTI9,INLST9) ; %
WRITE(PRINT,FMT11) ; %
WRITE(PRINT,FMT12) ; %
WRITE(PRINT,FMT13) ; %
WRITE(PRINT,FMTI12,INLST12) ; %
FOR T ← 1 STEP 1 UNTIL TT DO %
BEGIN %
              STABCHART(OSB1S,OSB2S,OSB3S,OSA1C,OSA2C,OSA3C,
                        ACB1S,ACB2S,ACB3S,ACA1C,ACA2C,ACA3C,
                        NNN,T,AMPLITUDE,NUMBER) ; %
              DAMPING(DB1S,DB2S,DB3S,N1S,N2S,N3S,AC1,AC2,AC3,
                      ACCMAX,DEK,NUMBER,T ) ; %
WRITE(PRINT[PAGE]) ; %
WRITE(PRINT,FMT6) ; %
WRITE(PRINT,FMT1) ; %
WRITE(PRINT,FMT01,LST1) ; %
WRITE(PRINT,FMT4) ; %
```

```
WRITE(PRINT,FMT5) ; %
WRITE(PRINT,FMT05,LST5) ; %
WRITE(PRINT,FMT21) ; %
WRITE(PRINT,FMT22) ; %
WRITE(PRINT,FMTOEXP,LSTEXP) ; %
WRITE(PRINT[PAGE]) ; %
WRITE(PRINT,FMT3) ; %
FOR JJ ← 0 STEP 1 UNTIL NN DO
WRITE(PRINT,FMT03,LST3) ; %
WRITE(PRINT[PAGE]) ; %
WRITE(PRINT,FMT17) ; %
WRITE(PRINT,FMT14) ; %
WRITE(PRINT,FMT19) ; %
FOR JJ ← 0    STEP 1 UNTIL NNN - 1 DO %
WRITE(PRINT,FMT07,LST7 ) ; %
WRITE(PRINT,FMT17) ; %
WRITE(PRINT,FMT15) ; %
WRITE(PRINT,FMT19) ; %
FOR JJ ← 0    STEP 1 UNTIL NNN - 1 DO %
WRITE(PRINT,FMT07,LST8 ) ; %
WRITE(PRINT[PAGE]) ; %
WRITE(PRINT,FMT17) ; %
WRITE(PRINT,FMT16) ; %
WRITE(PRINT,FMT19) ; %
FOR JJ ← 0    STEP 1 UNTIL NNN - 1 DO %
WRITE(PRINT,FMT07,LST9 ) ; %
WRITE(PRINT,FMT18) ; %
WRITE(PRINT,FMT14) ; %
WRITE(PRINT,FMT20) ; %
FOR JJ ← 1 STEP 1 UNTIL N1S DO %
            WRITE(PRINT,FMTU7D,LSD7 ) ; %
WRITE(PRINT[PAGE]) ; %
WRITE(PRINT,FMT18) ; %
WRITE(PRINT,FMT15) ; %
WRITE(PRINT,FMT20) ; %
FOR JJ ← 1 STEP 1 UNTIL N2S DO %
            WRITE(PRINT,FMTU7D,LSD8 ) ; %
```

```
WRITE(PRINT,FMT18) ; %
WRITE(PRINT,FMT16) ; %
WRITE(PRINT,FMT20) ; %
FOR JJ ← 1 STEP 1 UNTIL N3S DO %
                WRITE(PRINT,FMT07D,LSD9 ) ; %
%
END ;%
END ; %
END.
```

INPUT DATA

COLUMN VARIABLES

LENGTH (IN)	WIDTH (IN)	THICKNESS (IN)	DENSITY (LBM/FT*3)	YOUNG S MODULUS (LB/IN*2)
34.813	1.000	0.0625	485.0	2.9@+07

END MASS VARIABLES

END MASS (LB)	ECCENTRICITY (IN)	MOMENT OF INERTIA (LBM FT*2)
0.00	0.00	0.0000

OUTPUT DATA

NATURAL FREQUENCY NUMBER	NATURAL FREQUENCY (CYCLES PER SECOND)
1	1.67

MATHIEU S EQUATION

T (T)	COS(ΩT)×T(T)	T(T)
1.00	5.4146@-01	1.1025@+02

EXPERIMENTAL DATA

DAMPING DECREMENT

0.022

X (IN.)	MODE SHAPE RELATIVE DEFLECTION
0.00	0.00
1.39	-0.03
2.79	-0.11
4.18	-0.24
5.57	-0.42
6.96	-0.64
8.36	-0.90
9.75	-1.20
11.14	-1.54
12.53	-1.90
13.93	-2.30
15.32	-2.72
16.71	-3.17
18.10	-3.63
19.50	-4.11
20.89	-4.61
22.28	-5.12
23.67	-5.65
25.07	-6.18
26.46	-6.71
27.85	-7.26
29.24	-7.80
30.64	-8.35
32.03	-8.90
33.42	-9.45
34.81	-10.00

UNDAMPED
PRINCIPAL INSTABILITY REGION

BASE ACCELERATION (FT./SEC*2)	LOWER INSTABILITY BOUND	BASE ACCELERATION (FT./SEC*2)	UPPER INSTABILITY BOUND
0.0000@+00	1.00000	0.0000@+00	1.00000
3.0602@-01	0.99962	3.0648@-01	1.00038
6.1158@-01	0.99925	6.1342@-01	1.00075
9.1668@-01	0.99887	9.2083@-01	1.00113
1.2213@+00	0.99850	1.2287@+00	1.00151
1.5255@+00	0.99813	1.5370@+00	1.00189
1.8293@+00	0.99775	1.8458@+00	1.00227
2.1325@+00	0.99738	2.1551@+00	1.00264
2.4354@+00	0.99701	2.4648@+00	1.00302

UNDAMPED
SECOND INSTABILITY REGION

BASE ACCELERATION (FT./SEC*2)	LOWER INSTABILITY BOUND	BASE ACCELERATION (FT./SEC*2)	UPPER INSTABILITY BOUND
0.0000@+00	0.50000	0.0000@+00	0.50000
7.6562@-02	0.50000	7.6563@-02	0.50000
1.5312@-01	0.50000	1.5313@-01	0.50000
2.2969@-01	0.50000	2.2969@-01	0.50000
3.0625@-01	0.50000	3.0625@-01	0.50000
3.8281@-01	0.50000	3.8281@-01	0.50000
4.5937@-01	0.50000	4.5938@-01	0.50000
5.3594@-01	0.50000	5.3594@-01	0.50000
6.1250@-01	0.50000	6.1250@-01	0.50000

UNDAMPED
THIRD INSTABILITY REGION

BASE ACCELERATION (FT./SEC*2)	LOWER INSTABILITY BOUND	BASE ACCELERATION (FT./SEC*2)	UPPER INSTABILITY BOUND
0.0000@+00	0.33333	0.0000@+00	0.33333
3.4028@-02	0.33333	3.4028@-02	0.33333
6.8056@-02	0.33333	6.8056@-02	0.33333
1.0208@-01	0.33333	1.0208@-01	0.33333
1.3611@-01	0.33333	1.3611@-01	0.33333
1.7014@-01	0.33333	1.7014@-01	0.33333
2.0417@-01	0.33333	2.0417@-01	0.33333
2.3819@-01	0.33333	2.3819@-01	0.33333
2.7222@-01	0.33333	2.7222@-01	0.33333

DAMPED
PRINCIPAL INSTABILITY REGION

BASE ACCELERATION (FT./SEC*2)	LOWER INSTABILITY BOUND	UPPER INSTABILITY BOUND
2.8518@+00	1.00000	1.00000
1.9518@+01	0.97600	1.02343
3.6185@+01	0.95468	1.04335
5.2852@+01	0.93296	1.06282
6.9518@+01	0.91073	1.08193
8.6185@+01	0.88796	1.10069
1.0285@+02	0.86460	1.11914
1.1952@+02	0.84059	1.13728
1.3619@+02	0.81588	1.15514

DAMPED
SECOND INSTABILITY REGION

BASE ACCELERATION (FT./SEC*2)	LOWER INSTABILITY BOUND	UPPER INSTABILITY BOUND
3.4079@+01	0.49810	0.49839
5.0745@+01	0.49259	0.49959
6.7412@+01	0.48633	0.49978
8.4079@+01	0.47836	0.49986
1.0075@+02	0.46850	0.49991
1.1741@+02	0.45662	0.49993
1.3408@+02	0.44255	0.49995
1.5075@+02	0.42606	0.49996
1.6741@+02	0.40686	0.49997

DAMPED
THIRD INSTABILITY REGION

BASE ACCELERATION (FT./SEC*2)	LOWER INSTABILITY BOUND	UPPER INSTABILITY BOUND
7.7925@+01	0.32529	0.32682
9.4591@+01	0.31972	0.32485
1.1126@+02	0.31270	0.32223
1.2792@+02	0.30353	0.31922
1.4459@+02	0.29144	0.31589
1.6126@+02	0.27534	0.31226
1.7792@+02	0.25342	0.30835
1.9459@+02	0.22231	0.30417
2.1126@+02	0.17420	0.29974

OUTPUT DATA

NATURAL FREQUENCY NUMBER	NATURAL FREQUENCY (CYCLES PER SECOND)
2	10.43

MATHIEU S EQUATION

T (T)	COS(ΩT)×T(T)	T(T)
1.00	2.9807@+00	4.2962@+03

EXPERIMENTAL DATA

DAMPING DECREMENT

0.010

X (IN.)	MODE SHAPE RELATIVE DEFLECTION
0.00	0.00
1.39	-0.17
2.79	-0.62
4.18	-1.28
5.57	-2.10
6.96	-3.01
8.36	-3.94
9.75	-4.84
11.14	-5.65
12.53	-6.33
13.93	-6.83
15.32	-7.13
16.71	-7.20
18.10	-7.01
19.50	-6.58
20.89	-5.89
22.28	-4.97
23.67	-3.82
25.07	-2.47
26.46	-0.96
27.85	0.70
29.24	2.46
30.64	4.30
32.03	6.18
33.42	8.09
34.81	10.00

UNDAMPED
PRINCIPAL INSTABILITY REGION

BASE ACCELERATION (FT./SEC*2)	LOWER INSTABILITY BOUND	BASE ACCELERATION (FT./SEC*2)	UPPER INSTABILITY BOUND
0.0000@+00	1.00000	0.0000@+00	1.00000
1.1885@+01	0.99794	1.1983@+01	1.00208
2.3672@+01	0.99589	2.4067@+01	1.00417
3.5363@+01	0.99386	3.6252@+01	1.00628
4.6959@+01	0.99184	4.8541@+01	1.00840
5.8462@+01	0.98983	6.0934@+01	1.01054
6.9873@+01	0.98784	7.3432@+01	1.01270
8.1192@+01	0.98587	8.6039@+01	1.01487
9.2422@+01	0.98391	9.8754@+01	1.01705

UNDAMPED
SECOND INSTABILITY REGION

BASE ACCELERATION (FT./SEC*2)	LOWER INSTABILITY BOUND	BASE ACCELERATION (FT./SEC*2)	UPPER INSTABILITY BOUND
0.0000@+00	0.50000	0.0000@+00	0.50000
2.9834@+00	0.50000	2.9835@+00	0.50000
5.9669@+00	0.50000	5.9669@+00	0.50000
8.9502@+00	0.50000	8.9504@+00	0.50000
1.1933@+01	0.49999	1.1934@+01	0.50000
1.4917@+01	0.49999	1.4917@+01	0.50000
1.7900@+01	0.49998	1.7901@+01	0.50000
2.0882@+01	0.49998	2.0885@+01	0.50000
2.3865@+01	0.49997	2.3868@+01	0.50001

UNDAMPED
THIRD INSTABILITY REGION

BASE ACCELERATION (FT./SEC*2)	LOWER INSTABILITY BOUND	BASE ACCELERATION (FT./SEC*2)	UPPER INSTABILITY BOUND
0.0000@+00	0.33333	0.0000@+00	0.33333
1.3260@+00	0.33333	1.3260@+00	0.33333
2.6520@+00	0.33333	2.6520@+00	0.33333
3.9779@+00	0.33333	3.9779@+00	0.33333
5.3039@+00	0.33333	5.3039@+00	0.33333
6.6299@+00	0.33333	6.6299@+00	0.33333
7.9558@+00	0.33333	7.9558@+00	0.33333
9.2818@+00	0.33333	9.2818@+00	0.33333
1.0608@+01	0.33333	1.0608@+01	0.33333

DAMPED
PRINCIPAL INSTABILITY REGION

BASE ACCELERATION (FT./SEC*2)	LOWER INSTABILITY BOUND	UPPER INSTABILITY BOUND
9.1758@+00	1.00000	1.00000
2.5842@+01	0.99580	1.00418
4.2509@+01	0.99277	1.00717
5.9176@+01	0.98981	1.01009
7.5842@+01	0.98686	1.01297
9.2509@+01	0.98390	1.01584
1.0918@+02	0.98095	1.01869
1.2584@+02	0.97799	1.02154
1.4251@+02	0.97502	1.02437

DAMPED
SECOND INSTABILITY REGION

BASE ACCELERATION (FT./SEC*2)	LOWER INSTABILITY BOUND	UPPER INSTABILITY BOUND
1.6264@+02	0.49916	0.49925
1.7930@+02	0.49848	0.49958
1.9597@+02	0.49800	0.49968
2.1264@+02	0.49753	0.49974
2.2930@+02	0.49704	0.49979
2.4597@+02	0.49653	0.49982
2.6264@+02	0.49599	0.49984
2.7930@+02	0.49542	0.49986
2.9597@+02	0.49482	0.49988

DAMPED
THIRD INSTABILITY REGION

BASE ACCELERATION (FT./SEC*2)	LOWER INSTABILITY BOUND	UPPER INSTABILITY BOUND
4.2412@+02	0.32880	0.32947
4.4079@+02	0.32829	0.32927
4.5746@+02	0.32779	0.32905
4.7412@+02	0.32727	0.32881
4.9079@+02	0.32674	0.32855
5.0746@+02	0.32618	0.32828
5.2412@+02	0.32560	0.32799
5.4079@+02	0.32500	0.32770
5.5746@+02	0.32437	0.32740

OUTPUT DATA

NATURAL FREQUENCY NUMBER	NATURAL FREQUENCY (CYCLES PER SECOND)
3	29.21

MATHIEU S EQUATION

T (T)	COS(ΩT)×T(T)	T(T)
1.00	8.6011@+00	3.3683@+04

EXPERIMENTAL DATA

DAMPING DECREMENT

0.006

X (IN.)	MODE SHAPE RELATIVE DEFLECTION
0.00	0.00
1.39	-0.44
2.79	-1.56
4.18	-3.06
5.57	-4.64
6.96	-6.05
8.36	-7.07
9.75	-7.55
11.14	-7.41
12.53	-6.63
13.93	-5.26
15.32	-3.43
16.71	-1.31
18.10	0.91
19.50	2.99
20.89	4.74
22.28	5.97
23.67	6.55
25.07	6.41
26.46	5.53
27.85	3.95
29.24	1.78
30.64	-0.85
32.03	-3.78
33.42	-6.86
34.81	-10.00

UNDAMPED
PRINCIPAL INSTABILITY REGION

BASE ACCELERATION (FT./SEC*2)	LOWER INSTABILITY BOUND	BASE ACCELERATION (FT./SEC*2)	UPPER INSTABILITY BOUND
0.0000@+00	1.00000	0.0000@+00	1.00000
9.2460@+01	0.99409	9.4696@+01	1.00604
1.8277@+02	0.98830	1.9172@+02	1.01220
2.7102@+02	0.98263	2.9117@+02	1.01850
3.5728@+02	0.97707	3.9315@+02	1.02494
4.4163@+02	0.97162	4.9777@+02	1.03152
5.2415@+02	0.96627	6.0514@+02	1.03824
6.0489@+02	0.96103	7.1538@+02	1.04512
6.8393@+02	0.95589	8.2863@+02	1.05216

UNDAMPED
SECOND INSTABILITY REGION

BASE ACCELERATION (FT./SEC*2)	LOWER INSTABILITY BOUND	BASE ACCELERATION (FT./SEC*2)	UPPER INSTABILITY BOUND
0.0000@+00	0.50000	0.0000@+00	0.50000
2.3390@+01	0.50000	2.3391@+01	0.50000
4.6779@+01	0.49999	4.6782@+01	0.50000
7.0163@+01	0.49997	7.0174@+01	0.50001
9.3541@+01	0.49994	9.3567@+01	0.50001
1.1691@+02	0.49991	1.1696@+02	0.50002
1.4027@+02	0.49987	1.4036@+02	0.50003
1.6362@+02	0.49982	1.6376@+02	0.50004
1.8695@+02	0.49976	1.8716@+02	0.50005

UNDAMPED
THIRD INSTABILITY REGION

BASE ACCELERATION (FT./SEC*2)	LOWER INSTABILITY BOUND	BASE ACCELERATION (FT./SEC*2)	UPPER INSTABILITY BOUND
0.0000@+00	0.33333	0.0000@+00	0.33333
1.0396@+01	0.33333	1.0396@+01	0.33333
2.0792@+01	0.33333	2.0792@+01	0.33333
3.1187@+01	0.33333	3.1187@+01	0.33333
4.1583@+01	0.33333	4.1583@+01	0.33333
5.1978@+01	0.33333	5.1978@+01	0.33333
6.2373@+01	0.33333	6.2373@+01	0.33333
7.2768@+01	0.33333	7.2768@+01	0.33333
8.3162@+01	0.33332	8.3162@+01	0.33332

DAMPED
PRINCIPAL INSTABILITY REGION

BASE ACCELERATION (FT./SEC*2)	LOWER INSTABILITY BOUND	UPPER INSTABILITY BOUND
1.4958@+01	1.00000	1.00000
1.2607@+02	0.99198	1.00796
2.3718@+02	0.98477	1.01500
3.4829@+02	0.97753	1.02197
4.5940@+02	0.97024	1.02890
5.7051@+02	0.96290	1.03577
6.8162@+02	0.95551	1.04260
7.9274@+02	0.94805	1.04938
9.0385@+02	0.94054	1.05612

DAMPED
SECOND INSTABILITY REGION

BASE ACCELERATION (FT./SEC*2)	LOWER INSTABILITY BOUND	UPPER INSTABILITY BOUND
3.4228@+02	0.49950	0.49954
4.5339@+02	0.49847	0.49985
5.6450@+02	0.49749	0.49991
6.7561@+02	0.49633	0.49994
7.8672@+02	0.49497	0.49995
8.9784@+02	0.49342	0.49997
1.0089@+03	0.49166	0.49997
1.1201@+03	0.48969	0.49998
1.2312@+03	0.48751	0.49998

DAMPED
THIRD INSTABILITY REGION

BASE ACCELERATION (FT./SEC*2)	LOWER INSTABILITY BOUND	UPPER INSTABILITY BOUND
9.7194@+02	0.33018	0.33057
1.0830@+03	0.32919	0.33008
1.1942@+03	0.32812	0.32950
1.3053@+03	0.32693	0.32885
1.4164@+03	0.32560	0.32814
1.5275@+03	0.32411	0.32739
1.6386@+03	0.32246	0.32659
1.7497@+03	0.32062	0.32574
1.8608@+03	0.31859	0.32485

LITERATURE CITED

1. S. P. Timoshenko and J. M. Gere, Theory of Elastic Stability, McGraw-Hill, New York, 1961, pp. 100-107.

2. J. J. Stoker, "On the Stability of Mechanical Systems," Communications on Pure and Applied Mathematics, Vol. VIII, 1955, pp. 133-142.

3. A. M. Lyapunoff, "Problème général de la stabilité du movement," Ann. Fac. Sci. Univ. Toulouse (2) 9, 204-474 (1907); reprinted in the Annals of Mathematics Studies 17, (Univ. Press, Princeton, 1949).

4. W. T. Koiter, "Elastic Stability and Post Buckling Behavior," Collected paper in Nonlinear Problems by R. E. Langer, University of Wisconsin Press, 1963, pp. 257-275.

5. I. G. Malkin, Theory of Stability of Motion, United States Atomic Energy Commission, Office of Technical Information, Translation Number AEC-tr-3352.

6. N. M. Beliaev, "Stability of Prismatic Rods Subjected to Variable Longitudinal Forces," Collection of Papers: Engineering Constructions and Structural Mechanics (Inzhenernye sooruyheniia i stroitel' naia mekhanika), Put', Leningrad, 1924, pp. 149-167.

7. N. W. McLachlan, Theory and Application of Mathieu Functions, Dover Publications, Inc., New York, 1964.

8. E. A. Beilin and G. U. Dzhanelidze, "Survey of Work on the Dynamic Stability of Elastic Systems," Prikl. Mat. i Mekhan. 16(5), 635-648, 1952. (Available in English as ASTIA No. AD-264148).

9. V. V. Bolotin, Dynamic Stability of Elastic Systems, Gos. Iz. Tekh.-Teor. Lit. Moscow, 1956. (English translation by V. I. Weingarten et al., Holden-Day, San Francisco, 1964.)

10. J. H. Somerset and R. M. Evan-Iwanowski, "Experiments on Parametric Instability of Columns," Proceedings, Second Southeastern Conference on Theoretical and Applied Mechanics, Atlanta, Georgia, March, 1964, pp. 503-525.

11. H. A. Evensen and R. M. Evan-Iwanowski, "Effects of Longitudinal Inertia Upon the Parametric Response of Elastic Columns," Journal of Applied Mechanics, The American Society of Mechanical Engineers, March, 1966, pp. 141-148.

12. V. I. Weingarten, "Experimental Investigation of the Dynamic Stability of a Rod," TDR-269 (4560-40)-3, Aerospace Corporation, El Segundo, California, February 28, 1964.

13. Terry Farrell, "Parametric Resonance of Elastic Columns," AIAA Student Journal, Vol. 3, No. 3, October 1965, pp. 100-104.

14. I. S. Sokolnikoff, Mathematical Theory of Elasticity, McGraw-Hill, New York, 1956, pp. 413-414.

15. S. D. Conte, Elementary Numerical Analysis, McGraw-Hill, New York, 1965, pp. 40-41.